



Unveiling high concentrations of small microplastics (11–500 μm) in surface water samples from the southern Weddell Sea off Antarctica

Clara Leistenschneider^{a,b,*}, Fangzhu Wu^b, Sebastian Primpke^b, Gunnar Gerdts^b, Patricia Burkhardt-Holm^a

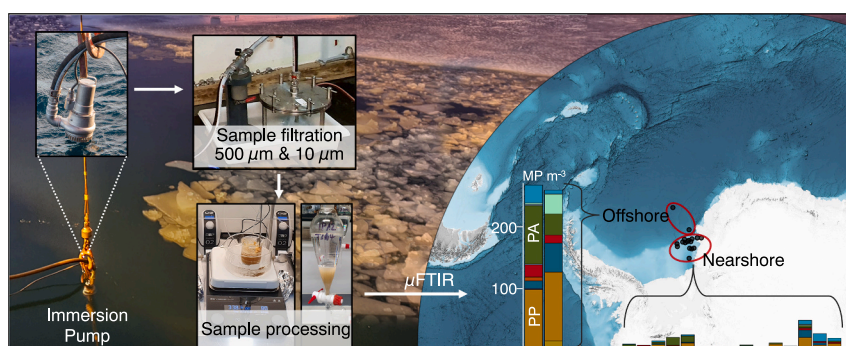
^a Man-Society-Environment Program, Department of Environmental Sciences, University of Basel, Vesalgasse 1, 4051 Basel, Switzerland

^b Shelf Sea System Ecology, Alfred Wegener Institute Helmholtz Centre for Polar and Marine Research, Kurpromenade 201, 27498 Helgoland, Germany

HIGHLIGHTS

- Study of small microplastics (11–500 μm) in the southern Weddell Sea off Antarctica
- Surface water sampled using a custom-designed sampling and filtration system
- High concentrations found with >98 % of all microplastics being 11–300 μm in size
- Distribution patterns may be influenced by local currents and/or sea ice conditions.

GRAPHICAL ABSTRACT



ARTICLE INFO

Editor: Damià Barceló

Keywords:

Small microplastics
Southern Weddell Sea
Antarctica
Seawater surface
FTIR

ABSTRACT

Recent studies have highlighted the prevalence of microplastic (MP) pollution in the global marine environment and these pollutants have been found to contaminate even remote regions, including the Southern Ocean south of the polar front. Previous studies in this region have mostly focused on MPs larger than 300 μm , potentially underestimating the extent of MP pollution. This study is the first to investigate MPs in marine surface waters south of the polar front, with a focus on small MPs 500–11 μm in size. Seventeen surface water samples were collected in the southern Weddell Sea using an in-house-designed sampling system. The analysis of the entire sample using micro-Fourier transform infrared spectroscopy (μFTIR) with focal plane array (FPA) detection revealed the presence of MPs in all samples, with the vast majority of the MPs detected being smaller than 300 μm (98.3 %). The mean concentration reached 43.5 (\pm 83.8) MPs m^{-3} , with a wide range from 0.5 to 267.2 MPs m^{-3} . The samples with the highest concentrations differed from the other samples in that they were collected north of the continental slope and the Antarctic Slope Current. Sea ice conditions possibly also influenced these varying concentrations. This study reports high concentrations of MPs compared to other studies in the region. It emphasizes the need to analyze small MPs, down to a size of 11 μm or even smaller, in the Antarctic Treaty Area to gain a more comprehensive understanding of MP pollution and its potential ecological impacts.

* Corresponding author at: Man-Society-Environment Program, Department of Environmental Sciences, University of Basel, Vesalgasse 1, 4051 Basel, Switzerland.

<https://doi.org/10.1016/j.scitotenv.2024.172124>

Received 22 February 2024; Received in revised form 27 March 2024; Accepted 29 March 2024

Available online 31 March 2024

0048-9697/© 2024 The Authors. Published by Elsevier B.V. This is an open access article under the CC BY license (<http://creativecommons.org/licenses/by/4.0/>).

1. Introduction

In recent decades, growing concern has emerged about the prevalence and impact of microplastics (MP; particles <5 mm) in marine ecosystems as they have been found to be ubiquitous around the globe (Arthur et al., 2009; Bergmann et al., 2017). These durable and pervasive environmental contaminants often contain chemical additives introduced during plastic production and have been shown to adsorb and transport hydrophobic persistent organic pollutants (POPs) and heavy metals from their surrounding environment and to transfer them to biota when ingested (Batel et al., 2016; Cao et al., 2021; Wang et al., 2024).

The global dispersion and transport of these lightweight materials by ocean currents and winds (Evangelidou et al., 2020; Howell et al., 2012; Isobe et al., 2014) position this issue as one that transcends local, national, and international boundaries and MPs have been identified in a wide range of marine habitats, from densely populated coastal areas to remote regions (e.g. Abel et al., 2021; Gündoğdu, 2022; Mishra et al., 2021).

Even Antarctica and the adjacent Southern Ocean - defined here as the ocean south of the 60°S latitude - faces emerging challenges from MP pollution (e.g. Gurumoorthi and Luis, 2023; Rota et al., 2022; Waller et al., 2017). MP contamination has been evidenced in different environmental matrices in Antarctica and the Southern Ocean including surface and subsurface seawater (Cincinelli et al., 2017; Leistschneider et al., 2021; S. Zhang et al., 2022), sediments (Cunningham et al., 2020; Munari et al., 2017; Van Cauwenberghe et al., 2013), sea ice cores (Kelly et al., 2020), glacier surface samples (González-Pleiter et al., 2021), snow (Aves et al., 2022) and freshwater (González-Pleiter et al., 2020). There is evidence that MP pollution originate from local sources such as shipping (Lacerda et al., 2019; Leistschneider et al., 2021) and research stations (Cincinelli et al., 2017; González-Pleiter et al., 2021; Munari et al., 2017). However, even if the strong Antarctic Circumpolar Current (ACC) is considered to be a barrier that mitigates passive north-south dispersal of drifting material and biota, MPs could be additionally transported into the Southern Ocean from regions further north, crossing the ACC via ocean eddies and storm-driven surface waves (Fraser et al., 2018, 2016; Waller et al., 2017). Once present in the Southern Ocean south of the ACC, MPs might get trapped and accumulate in the region (Lacerda et al., 2019; Mountford and Maqueda, 2021).

Although marine MP concentrations in Antarctica are relatively low compared to other global regions (Gurumoorthi and Luis, 2023), MP ingestion has been documented in several Antarctic biota from different levels of the food chain including several penguin species, krill and salps, benthic invertebrates and fish (e.g. Bergami et al., 2023; Fragão et al., 2021; Primpke et al., 2024; Sfriso et al., 2020; Wilkie Johnston et al., 2023; M. Zhang et al., 2022). However, in Antarctic fur seals and Emperor penguins MP ingestion could not be evidenced (García-Garin et al., 2020; Leistschneider et al., 2022) indicating low levels in certain regions. Yet, Antarctic biota, adapted to isolation, extreme cold, and seasonality, including periods of food scarcity, are especially vulnerable to environmental pollutants, revealing traits such as slow metabolisms, limited detoxification pathways, reliance on lipid storage, and long lifespans, face heightened risks from bioaccumulation, especially of lipophilic contaminants (Peck, 2018; Pörtner, 2006; Strobel et al., 2015). The region's short food chains, heavily reliant on Antarctic krill and silverfish, further amplify these risks.

It has been shown that environmental MP concentrations typically increase with decreasing particle size (Abel et al., 2022; Covernton et al., 2019; Pabortsava and Lampitt, 2020), and there are concerns that these more abundant smaller MPs pose a more significant risk to aquatic biota (Kögel et al., 2020).

Despite that, the majority of studies investigating MPs in waters of the Southern Ocean have analyzed MPs >300 µm, with only few studies including MPs down to sizes of 60 µm (Cincinelli et al., 2017) and 100

µm (Cunningham et al., 2022; Pakhomova et al., 2022). Moreover, most studies examining MPs in abiotic environmental matrices of the Southern Ocean have mainly focussed on marine waters in areas with significant human activity (Rota et al., 2022). Less is known about remote regions, such as the southern Weddell Sea. Two studies analyzed MPs >300 µm (Leistschneider et al., 2021) and > 100 µm (Cunningham et al., 2022). However, the latter did not report MP concentrations for water samples and only sampled volumes of a few liters per sample, which may not provide reliable data, particularly for such remote regions (Cowger et al., 2020; Lofty et al., 2023).

In this study, we examine the presence of MPs down to a size of 11 µm surface waters of southern Weddell Sea, a particular remote region of the Southern Ocean. The principal aim is to bridge a significant gap in our understanding of MP pollution in the Southern Ocean, with a particular focus on small MPs (11–500 µm; Roscher et al., 2021) in the surface waters of the Weddell Sea. Through a comprehensive analysis of small MPs, this paper aims to provide valuable insights that will inform future research and conservation efforts in the region, contributing to a broader understanding of MP pollution within the Antarctic Treaty Area.

2. Material and methods

2.1. Sampling area

Surface water samples were collected during expedition *PS124* aboard the research vessel (RV) *Polarstern* to the southern Weddell Sea. The expedition took place from February to March 2021, departing from and returning to Stanley, Falkland Islands (Hellmer and Holtappels, 2021). The sampling stations for this study were opportunistic and based on the stations planned by the primary users. Two of the 17 samples (Samples 1 and 2) were collected in the offshore region north of the continental slope, and one sample (Sample 17) was collected in the crack behind iceberg A74 (area 1270 km, crack length ~ 100 km), which calved on 26 February 2021 from the Brunt Ice Shelf. Most sampling stations were, however, located in the shallower waters over the continental shelf, delimited by the 1000-m isobath (Fig. 1).

The sampling region is mainly influenced by the westward-flowing Antarctic Slope Current (ASC), which circumnavigates Antarctica parallel to the continental slope with its path approximately following the 1000-m isobath (Huneke et al., 2022; Morrison et al., 2020), separating the shallower waters over the continental shelf from the deeper offshore areas (Fig. 1a).

2.2. Sampling procedure

2.2.1. Sample collection

Seventeen surface water samples were collected between latitudes 70°S and 77°S by means of an in-house-designed sampling system, targeting MPs down to a size of 10 µm. This system used a mobile immersion pump (CH432, HOMA, Germany) to pump seawater into a 1 m³ stainless steel tank (PC1000A4, Inox Behälter GmbH, Germany) via a PTFE hose (Ø 2"; length: 15 m; TUFLON PTFE CHEM, 143487, Industriebedarf CASTAN GmbH; Fig. S1a).

The immersion pump, attached to the PTFE hose, was deployed from the starboard side using the on-board crane while the vessel was stationary. The crane was extended to its maximum reach, achieving a lateral distance of approximately 5 m from the vessel's hull. Depending on the sea state, the immersion pump was then submerged between 30 and 80 cm. To avoid cross-contamination, all components were rinsed and primed by pumping seawater from the respective station through the sampling system before taking the final sample (for more details see Section 2.5 Quality Assurance/Quality Control (QA/QC)). Finally, the sample was collected by pumping approximately 1 m³ of seawater into the primed tank (taking approximately 2.5 min).

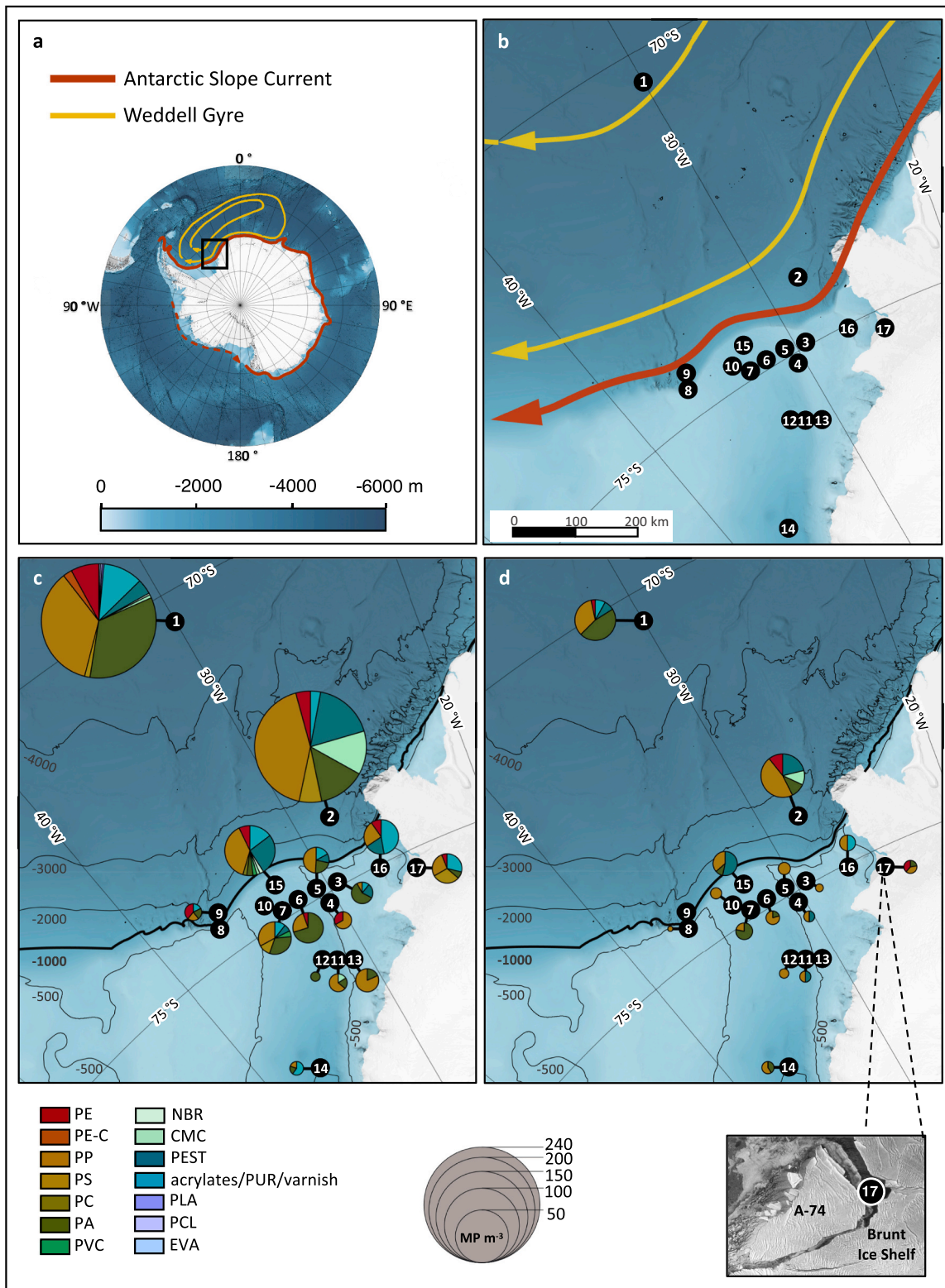


Fig. 1. Sampling Sites and Microplastic (MP) Occurrence in Surface water samples from the southern Weddell Sea. (a) Overview of Antarctica and the Southern Ocean with the study area marked by the black square and (b) map of the study area with the sampling sites (1–17). The red line in (a) and (b) indicates the Antarctic Slope Current while the yellow lines indicate the Weddell Gyre, adapted from (Huneke et al., 2023; Thompson et al., 2018). (c) Polymer composition and estimated concentrations per m^3 for MP particles. (d) Polymer composition and estimated concentrations m^3 for elongated MPs. Isobaths are indicated by black lines, with the 1000-m isobath depicted as thick black, marking the continental slope. MP concentrations (m^{-3}) at each sampling site are indicated by the size of the pie charts. The polymer types are color-coded and include PE (polyethylene), PE-C (polyethylene-chlorinated), PP (polypropylene), PS (polystyrene), PC (polycarbonate), PA (polyamide), PVC (polyvinyl chloride), NBR (nitrile rubber), CMC (chemically modified cellulose), PEST (polyester), acrylates/PUR/varnish (acrylates/polyurethane/varnish/lacquer), PLA (polylactic acid), PCL (polycaprolactone), and EVA (ethylene vinyl acetate). An inset of the TerraSAR-X satellite image (courtesy of the German Aerospace Center, DLR) shows the gap between iceberg A74 and the Brunt Ice Shelf on March 13, 2021. The maps were produced using Quantarctica (v3.1; Matsuoka et al., 2021) with bathymetry according to IBCSO (v2; Dorschel et al., 2022).

2.2.2. Sample filtration

The collected seawater was filtered directly from the sampling tank using a pneumatic pump (E15TTT-F4, Almatec Maschinenbau GmbH, Germany) to lead the seawater through the downstream filtration steps. This included a 500 μm stainless steel cartridge filter (01WTGD05, Wolftechnik, Germany) to pre-filter the sample and remove particles $>500 \mu\text{m}$, minimizing the potential for clogging in the subsequent filtration stage and facilitating MP analyses. The water was then led through a stainless-steel pressure filter holder (H293SSI, Pieper Filter GmbH, Germany) with a 10 μm stainless steel filter (\varnothing 293 mm; 1076420, Körner, Germany) to collect particles between 11 μm and 500 μm . The tank, the pneumatic pump and the filter holders were connected in series via $\frac{1}{2}$ " PTFE-hoses (TUFLON PTFE CHEM, 143478, Industriebedarf CASTAN GmbH; Fig. S1b). A flowmeter (8188-20, Gardena, Germany) was installed to the outlet of the stainless-steel pressure filter holder to measure the filtered volume. During the filtration process, the sampled seawater was stirred in the tank using a stirrer (SRT9-1500, Inox Behälter GmbH, Germany) permanently installed to the tank. This was done to dislodge particles that might otherwise adhere to the walls of the tank. After the filtration process, the filter holder containing the 10 μm filter was opened by one researcher, while a second researcher immediately folded the filter in half twice, to avoid airborne sample contamination. The folded 10 μm filters with the suspended solids were wrapped in Milli-Q (Millipore, Milli-Q Gradient A10 purification system) rinsed aluminum foil and stored in Milli-Q rinsed aluminum boxes at $-20 \text{ }^\circ\text{C}$.

While the focus of this study was on small MPs, the 500 μm stainless steel cartridge filter was nevertheless examined for MPs $>500 \mu\text{m}$ to cover the entire size range of MPs. For this purpose, the cartridge filter was rinsed with Milli-Q and the rinse water as well as the cartridge filter itself were examined under a stereomicroscope (Olympus SZ61, Tokyo, Japan, magnification 6.7–45 \times) on board. The cartridge filter and rinse water were generally very clear with little visible particulate material, and no suspicious particles were detected. Although no putative MPs $>500 \mu\text{m}$ were detected in the cartridge filter, it is noteworthy that MPs $>500 \mu\text{m}$ were nevertheless detected on the subsequent 10 μm filter, which targeted small MPs with a size of 11–500 μm . These are most likely MPs exceeding the length of 500 μm but with a width, or in the case of elongated MPs, a diameter, $<500 \mu\text{m}$.

2.3. Sample processing

After being shipped frozen on RV *Polarstern* to the Alfred Wegener Institute (AWI) in Bremerhaven, Germany, and from there on RV *Uthörn* to AWI Helgoland, samples were processed in the laboratory, dedicated to MP research. To isolate MPs and remove other organic and inorganic material, several treatment steps were needed prior to chemical particle identification via FPA- μFTIR . These treatment steps included (1) the detachment of collected suspended solids from the sampling filters (Roscher et al., 2021), (2) the oxidative digestion of natural organic material (Tagg et al., 2017), and (3) the removal of high-density inorganic material applying density separation (Quinn et al., 2017).

2.3.1. Detachment of suspended solids from the sampling filters

Prior to isolation of MPs from the sample matrix, the particulate material collected on the large sample filters was transferred to small 47 mm stainless steel filters (10 μm , GKD, Germany) to facilitate subsequent processing steps. The folded sample filters were thawed and rinsed from the outside to remove any adhering particles. The filter meshes were then cut into approximately 32 pieces on a stainless-steel dissection tray using steel scissors. The mesh pieces were transferred to a 1 L glass beaker and possible residues left on the dissecting tray were flushed into the same beaker using Milli-Q water and a PTFE-Squirt bottle. The mesh pieces were then incubated for 24 h in 0.1 % sodium dodecyl sulfate (SDS; w/v; Carl Roth, Germany) at $40 \text{ }^\circ\text{C}$ while being slightly shaken at 11 rpm. The next day, the mesh pieces were taken out

of the incubation solution individually and rinsed with Milli-Q and a PTFE-squirt bottle. Rinsed mesh pieces that appeared to be free of particulate material by the naked eye, were collected in a 1 L Erlenmeyer flask with an aluminum lid. The Erlenmeyer flask containing the rinsed mesh pieces was filled again with 500 mL of Milli-Q, shaken thoroughly by hand and the solution was filtered as described above. This additional rinsing procedure was repeated three times before three randomly selected mesh pieces were inspected for possible residues under a dissection microscope (Olympus SZX16, Olympus, Germany). If residues were present, the process was repeated until no residues were detected. The incubation and rinsing solutions were vacuum-filtered onto 47 mm stainless steel filters. The 47 mm filters were transferred to 150 mL glass beakers and covered with aluminum foil until the next treatment step.

2.3.2. Automated Fenton treatment

To perform the oxidative digestion and remove natural organic matter, Fenton's reagent was applied according to the protocol by Al-Azzawi et al. (2020) with minor modifications and the incorporation of a semi-automated approach to speed up the process and to allow parallel treatment of up to six samples (Fig. S2). The 150 mL beakers each containing a 47 mm filter with the samples, were placed in an ice bath, with a PTFE caged stirrer placed atop each filter inside the beakers, ensuring a consistent rotation of 70 rpm throughout the reaction. Following this, 15 mL of aqueous iron (II) sulfate (FeSO_4) solution (pH 3, 20 g/L; AppliChem GmbH, Germany) was introduced to each beaker using a glass pipette. This was subsequently followed by a gradual addition of 70 mL of 30 % H_2O_2 (01176.3110, Bernd Kraft GmbH, Germany) over a span of 10 min via automated dosing pumps (flow rate: 7 mL/min; SIMDOS 02 FEM 1.02 S, KNF DAC GmbH, Germany). Following the complete addition of reagents, the samples were allowed to stand for an additional 10 min to let the reaction complete and to permit the samples to cool. Continuous monitoring of the reaction temperature was conducted, with additional ice added to the ice bath as needed to prevent the temperature from exceeding $40 \text{ }^\circ\text{C}$. After a total of 20 min, 4 mL of sulfuric acid (95–97 %, for analyses, 100731, Merck, Germany) was added to dissolve the iron precipitates formed during the oxidation treatment. When the sample solution was clear again, taking approx. 30 s, 10 mL of 0.1 % (v/v) tween 20 (VWR International, France) was added to prevent particle aggregation and maintain the MPs in suspension. Immediately after, the samples were filtered onto new 47 mm stainless steel filters.

2.3.3. Density separation

2.3.3.1. Density separation using NaBr. Following the oxidative digestion of natural organic material, a density separation was performed to remove heavy inorganic material using a sodium bromide (NaBr) solution, according to the methodology by Abel et al. (2022). The NaBr solution with a density of approximately 1.56 g cm^{-3} was made by dissolving NaBr (99.5 % purity, Grüssing GmbH, Diagnostica Analytika, Germany; Quinn et al., 2017) in Milli-Q water. Using this solution and a PTFE squirt bottle, the samples were rinsed into glass separation funnels (50 mL, LabMarket GmbH, Germany). Prior to allowing the samples to settle, the separation funnels were shaken carefully by hand for 30 s. Any particles potentially adhering to the inner wall of the separation funnel and the PTFE lid were rinsed down and resuspended using additional NaBr solution from the PTFE squirt bottle. After 12 h, the lower solid and aqueous phase was drained. The separation funnel was then refilled with NaBr solution to the initial volume, shaken, and the entire process was repeated twice more, with the lower fraction being drained after 4 and 8 h, respectively. Afterwards, the remaining upper "MP-fraction" was drained, vacuum filtered onto 47 mm stainless steel meshes, and rinsed with approximately 200–300 mL of Milli-Q to eliminate NaBr residues. Finally, the samples were transferred from the filters to a 100 mL glass wide-neck bottle using Milli-Q and a PTFE squirt bottle and were stored

at 4 °C until subjected to the final filtration for μ FTIR-measurements.

By applying this protocol, originally applied on sediment samples (Abel et al., 2022), we were unable to purify three out of 17 samples. There was still a thick white layer on the surface of these samples in the separation funnel (Fig. S3a). These residues were found to contain diatoms (including genera such as *Asteromphalus*, *Corethron*, *Fragilaria*, *Thalassiosira*) and silicoflagellates (Fig. S4), in addition to unidentifiable “cloudy” material, as determined by light microscopy (Olympus SZX16, Olympus, Germany). Additional μ FTIR measurements conducted on small 50- μ L subsamples revealed a predominance of residues mainly consisting of natural polysaccharides, which could potentially originate from algae/diatoms or plant material, and further some keratinous particles, which were apparently not efficiently removed by the initially applied protocol (Table S1). Consequently, the affected samples were subjected to a second density separation.

2.3.3.2. Second density separation using LST FastFloat. The second density separation was performed using LST FastFloat (sodium heteropolytungstates dissolved in water; Central Chemical Consulting Pty Ltd., Australia) a water-based heavy liquid with a particularly low viscosity (10 cP at a density of 2.82 g cm⁻³). The LST FastFloat was diluted with Milli-Q to a density of 2 g cm⁻³. The density separation was conducted in the same manner as described for the first density separation.

Using LST FastFloat, all but one sample was successfully purified (Fig. S3a–d). For the sample that was not purified completely, the upper “MP-fraction” of the unpurified sample was divided into two parts: a “clear MP-fraction” and a “turbid MP-fraction,” with the latter being the uppermost fraction containing visible residues. The “clear MP-fraction” was treated identically to all other samples and analyzed via μ FTIR subsequently, whereas the “turbid MP-fraction” underwent visual inspection under a stereo microscope. Any particles identified visually as putative MPs were carefully transferred to a glass petri dish using fine tweezers. Afterwards, these particles were directly rinsed and filtered onto an Anodisc filter using Milli-Q (Millipore, Milli-Q Gradient A10 purification system) and a PTFE squirt bottle, for subsequent μ FTIR measurement.

2.4. Chemical identification of MPs

Following the two to three purification steps, samples were vacuum-filtered from the wide-neck bottles onto aluminum-oxide filters (Anodisc, Ø 25 mm; 0.2 μ m pore size, Whatman, UK) using a custom-made filtration device (Primpke et al., 2024). The wide-neck bottles were shaken carefully for sample homogenization just before transferring the sample solution to the filtration system. Depending on the sample, between two and 13 Anodisc filters were required to prevent filter overload and particle overlay. The wide-neck bottles were always carefully shaken to homogenize the samples before the sample solution was filtered onto the Anodisc filters. Nevertheless, all resulting subsamples/aliquots were measured via μ FTIR as it has been shown previously that extrapolation of individual subsamples can lead to significant over- or underestimations (Abel et al., 2021; Roscher et al., 2021). After filtration, the Anodisc filters were placed in glass Petri dishes and dried in a desiccator at 37 °C for a minimum of 48 h prior to measuring them with a μ FTIR-microscope (Hyperion 3000, connected to a Tensor 27 spectrometer; Bruker Optik GmbH, Germany), using a focal plane array (FPA) detector with a pixel size of 11.1 \times 11.1 μ m and the software OPUS 8.5 (Bruker Optics GmbH, Germany). For the measurements, the Anodisc filters were covered with a BaF₂-IR-window (Ø 25–0.2 mm, h: 22 \pm 0.1 mm, 25 40 006, Korth Kristalle GmbH, Germany) to keep all items within the focal plane of the FTIR microscope, and particularly enabling the detection of elongated particles (here referring to fiber-like MPs; Primpke et al., 2019). The FTIR microscope was equipped with a 3.5 \times IR objective and the lower detection limit was 11 μ m. Further, the following settings were applied: A spectral range of 3600–1250 cm⁻¹,

with 32 scans (n background scans: 64), a spectra resolution of 8 cm⁻¹, Blackman-Harris 3-term apodization and a zero-filling factor of 2. A grid of 22 \times 22 FPA measurement fields was applied to cover the filtration area. In a few cases, it was necessary to expand the grid to a size of 26 \times 26 to ensure all particles were covered.

MP analysis was performed using the following pipeline: The resulting FTIR spectra were processed with the software OPUS 8.5 before using the software tool siMPle (Primpke et al., 2020) for automated MP identification and quantification. We applied the reference database initially designed by Primpke et al. (2018) and later extended with plant cuticle material by (Roscher et al., 2022). Due to evidence of vessel-induced sample contamination in our previous study (Leistschneider et al., 2021), we extended the database further with spectra from ship paint references. These included paint flakes collected directly from RV *Polarstern* ($n = 45$) during expedition PS117 and PS124, and the same paints from AkzoNobel, International, freshly applied in the laboratory ($n = 165$), as detailed in our previous work (Leistschneider et al., 2021). For incorporation into the database spectra were subjected to a hierarchical cluster analysis according to Primpke et al. (2018), assigning the paint references to two additional polymer clusters.

Finally, image analysis via MPAPP (Primpke et al., 2019) was performed based on the spectral matching thresholds presented by (Lorenz et al., 2019) providing all data on polymer clusters (in the following denoted as “polymer type”), MP quantities, size classes and shapes (particles and elongated) of detected MPs in a tabular format. The reported size classes represent the longest lengths of the MPs (maximum ferret diameter). For elongated MPs, the minor dimension is fixed due to the selection rules of the MPAPP script as described in Primpke et al. (2019), which targets particles with a diameter typical for textile fibers and an aspect ratio of 3:1 or higher. As contributions from other sources cannot be completely excluded, the term elongated MPs is used rather than fibers. The size class of 11 μ m is exclusive to MP particles, as distinguishing between particles and elongated particles becomes infeasible at the lower detection limit of 11 μ m.

2.5. Quality Assurance/Quality Control (QA/QC)

To minimize sample contamination and to ensure the reliability of the results we followed meticulous QA/QC protocol. Researchers always wore 100 % cotton lab coats when handling the samples on board of RV *Polarstern* as well as in our home laboratory. A practice of clean hands was prioritized to the use of nitrile gloves, substantiated by findings from Witzig et al. (2020) showing that stearates or fatty leaches from nitrile gloves might be misidentified as synthetic polymers. Yet, nitrile gloves needed to be used due to safety reasons during Fenton's protocol (Section 2.3.2).

Materials used during sampling and sample processing were made of glass, steel, aluminum, or PTFE, the latter being a non-detectable synthetic polymer within the applied spectral range. All used materials were thoroughly air-blown (Airbrushgun Typ 180 with Airbrush compressor AF186, WilTec Wildanger Technik GmbH, Germany) and rinsed with Milli-Q before use. Sample processing was conducted under a laminar flow bench (ScanLaf Fortuna, 1800; LaboGene, Lillerød, Denmark) at all times to ensure a contamination-controlled environment and samples were covered with Milli-Q rinsed aluminum foil whenever a process had to be paused. Furthermore, all chemicals were filtered through glass microfiber filters (GF/F, Ø 47 mm, pore size: 0.7 μ m, VWR, Germany) to exclude potential particulate contaminants, except for the 95–97 % H₂SO₄ due to safety reasons. Further, the treatment step involving H₂SO₄ had to be conducted under a fume hood instead of the clean bench. However, we are confident that the procedural blanks, for which the same filters and treatment steps were applied, yet, without a real sample, will account for possible contamination during this and all other steps in the protocol. Procedural blanks were processed in parallel with each batch of 4–5 water samples.

During transport and onboard RV *Polarstern* Camlock couplings were used for the secure storage of hoses, pumps, filter holders, and the 1 m³ tank, protecting them from airborne contamination.

The sampling and filtration systems were primed with seawater from each respective station. Prior to sampling, seawater was pumped through the 2" PTFE hose, before attaching it to the steel tank, to first rinse the hose and immersion pump. Subsequently, the steel tank was primed, by attaching the PTFE hose with the immersion pump to the tank to fill it completely. The seawater was then discarded from the tank through a designated outlet and the actual sample was finally taken. After sampling and before each sample filtration from the 1 m³ tank, 100 L of the sampled seawater were pumped through the filtration setup to rinse and prime the system prior to inserting the filter.

Additionally, five field blanks were obtained on RV *Polarstern* post-sampling by exposing a 400 mL glass jar (Ø 82 mm) with 200 mL of Milli-Q on the working deck for a duration of 5 min. Yet, while field blanks taken on the working deck serve to identify potential microplastic contaminants originating from the RV, they cannot quantify the actual concentration of such contaminants in the surface water samples. The field blanks were stored frozen at -20 °C and in our home laboratory the field blanks were thawed, filtered directly onto Anodisc filters, and analyzed in the same manner as the water samples.

Due to our findings from a previous study, where shipborne contamination by ship paint fragments was observed, ship paint samples from RV *Polarstern* were taken for implementation to the database and spectral comparison. After initial data analysis and quality control of the received results particles identified as ship paint from the RV *Polarstern*, rubber type 3 (RT3) and acrylamides were excluded from our study. Evidence for inaccurate spectral matching or potential mis-identifications with lipids/stearates (Primpke et al., 2024; Witzig et al., 2020) was found after manual spectral evaluation of 100 randomly selected spectra from each of these polymer types (Section 4.3; Fig. S5).

2.6. Data evaluation

As described in Section 2.4, the treated sample material had to be divided into two to 13 subsamples per sample for Anodisc filtration prior to µFTIR analysis to avoid filter overload. To obtain MP counts for each sample, the number of MP identified of each polymer type within each subsample was summed. To account for possible contamination from sample processing, the numbers of MPs identified for each polymer type in the procedural blanks were averaged, and the number of MPs from the corresponding polymer type and size classes was subtracted from the MP count in each water sample. MP concentrations m⁻³ were calculated from the total number of MP per sample and the corresponding sample volume (supplementary information (SI), S1.xlsx). These steps were performed separately for MP particle data, elongated particle data, and combined total MP data.

To explore potential relationships between MP concentration and environmental variables (natural particle concentration; wind velocity, water temperature and conductivity obtained from the RVs system for underway data; sea ice coverage data from ice observations conducted from the RVs bridge (Haas et al., 2021); S1.xlsx) as well as geographic variables (latitude, longitude; S1.xlsx), correlation analysis was applied, using Spearman's rank correlation due to the non-normally distributed nature of our data (R Core Team, 2023).

3. Results

3.1. Blank samples

The procedural blanks contained a total of 55 MPs, ranging from 0 to 19 MPs per blank sample (mean ± SD, 11 ± 7.9) and assigned to 8 different polymer types (PP, PEST, PA, PE, PC, CMC, acrylates/PUR/varnish, EVA). In the five field blanks taken on the working deck of RV *Polarstern*, 54 MPs assigned to 6 polymer types were detected (PA, PE,

acrylates/PUR/varnish, PEST, rubber type 1 (RT1)). The MP count per field blank ranged from 5 to 16 MPs (mean ± SD, 10 ± 5.3 MPs) and the mean (± SD) MP deposition rate was estimated at 432 MPs min⁻¹ m⁻² (± 212.4 MPs min⁻¹ m⁻²). Further details regarding the blank samples can be found in the SI (Paragaph S1 and S1.xlsx).

3.2. MP concentrations, distribution, and polymer composition

In total, 14.22 m³ of surface water were sampled from the southern Weddell Sea, yielding a mean (± SD) volume of 0.84 (± 0.15) m³ per sample. At station 2, sampling was limited to 0.27 m³ due to problems with the sampling device. From all samples (n = 17), 561 MPs, including both particles and elongated particles, were identified using FPA-µFTIR measurements (S1.xlsx). After accounting for the mean MP numbers in the procedural blanks, the net count of MPs was 476.2, including 405.2 MP particles and 71 elongated MPs, suggesting that 15 % of all MPs were derived from contamination during sample processing.

The mean (± SD) concentration of total MPs was found to be 43.5 (± 83.8) MPs m⁻³, with MP items found in all samples, although two samples were free of MP particles and one sample was free of elongated MPs, respectively (Fig. 1). Samples collected offshore (Sample 1 and Sample 2) had significantly higher estimated MP concentrations (267.2 and 259.2 MPs m⁻³, respectively) compared to nearshore samples (range: 0.5–56.1 MPs m⁻³). While concentrations of elongated MPs were found to be an order of magnitude lower than MP particles, both shape categories still showed a similar distribution pattern (Fig. 1b and c; Table 1).

In terms of polymer composition, PP and PA were found to be the predominant polymer types in both shape categories (Table 1). PP particles showed a notable presence among the samples, with only one sample containing MP particles not containing PP, while PA particles showed a more variable contribution. For samples containing elongated MPs, PP was found in all samples. Conversely, PA, although less consistent, reached high concentrations in some samples, suggesting that its presence is specific to some samples rather than being evenly distributed. Details of the percentages of all polymer types are illustrated in boxplots (Fig. 2a and b). Looking at the polymer richness, 14 different polymer types were found, all of which were found among the MP particles, whereas fibers consisted of only six different polymer types. Samples collected offshore had a higher mean polymer richness than those collected nearshore (Table 1).

3.3. MP size distribution

Image analysis revealed a general trend where the number of MPs increases inversely with their size class, highlighting the dominance of smaller size classes among the observed MPs. We found that 98.3 % of the total MPs, including both MP particles and elongated MPs, are smaller than 300 µm, with 94.5 % smaller than 100 µm and 60.6 % smaller than 25 µm (Fig. S6). However, when looking at the different MP shapes separately, the trend seems to be less clear for elongated MPs.

For MP particles, a distinct pattern was observed with smaller MP particles being more abundant (Fig. 2c). Almost all MP particles were smaller than 200 µm (99.8 %). The smallest size class (11 µm) was present in all samples and accounted for 42.1 % of all MP particles, showing a consistent trend across samples with a median percentage of 40 % and a contribution ranging from 12.5 % to 72 % across all samples containing MP particles. Larger particles (>200 µm) were only present in the >500 µm size class, accounting for only 0.2 % of the MP particles.

Elongated MPs showed a less pronounced but still significant trend toward smaller sizes (Fig. 2d), with the 25–50 µm size class showing the highest median percentage (25 %). However, larger size classes were also present, with 12.6 % of elongated MPs exceeding 200 µm. The largest size class had a mean percentage of 10.32 %, indicating its occasional high presence, but the median percentage of 0 indicates that it was typically rare.

Table 1

Microplastic (MP) concentrations and polymer composition in the sampling area. The table presents MP concentration and polymer composition data for the entire sampling area and for nearshore and offshore sites for comparison. Polymer richness (n_{poi}) represents the number of polymer types identified. Polymer abbreviations are as follows: PE: polyethylene; PE-C: polyethylene-chlorinated; PP: polypropylene; PS: polystyrene; PC: polycarbonate; PA: polyamide; PVC: polyvinylchloride; NBR: nitrile rubber; CMC: chemically modified cellulose; PEST: polyester; acrylates/PUR/varnish: acrylates/polyurethane/varnish/lacquer; PLA: polylactide acid; PCL: polycaprolactone; EVA: ethylene vinyl acetate.

| | Total MPs | MP Particles | Elongated MPs |
|---|---|---|--|
| MP concentration [m^{-3}] | | | |
| Total region (mean \pm SD; range) | 43.5 \pm 83.8 (0.5–267.2) | 37.2 \pm 73.8 (0–237.2) | 6.3 \pm 10.1 (0–34.3) |
| Nearshore (mean \pm SD; range) | 14.2 \pm 14.1 (0.5–56.1) | 11.4 \pm 11.7 (0–45.4) | 2.8 \pm 2.7 (0–10.8) |
| Offshore (range) | 259.2–267.2 | 237.2–224.9 | 30.0–34.3 |
| n samples containing MP | 17 | 15 | 16 |
| Polymer composition | | | |
| n_{poi} total (mean \pm SD) | 14 (4.4 \pm 2.8) | 14 (4.1 \pm 3.1) | 6 (1.9 \pm 1.4) |
| n_{poi} nearshore (mean \pm SD) | 10 (3.7 \pm 2.0) | 10 (3.3 \pm 2.3) | 5 (1.5 \pm 0.9) |
| n_{poi} offshore (mean \pm SD) | 12 (9.5 \pm 3.5) | 12 (9.5 \pm 3.5) | 6 (5 \pm 0) |
| Dominant polymers (%) | PP (39.6 %), PA (23.4 %), PEST (11.2 %), acrylates/PUR/varnish (9.2 %), PE (6.1 %), CMC (2.7 %), PS (3.5 %) | PP (37 %), PA (26.2 %), acrylates/PUR/varnish (12 %), PEST (9.1 %), PE (6.8 %), PS (3.2 %), CMC (2.7 %), PE-C (1.2 %) | PP (46.8 %), PA (26.8 %), PEST (15.5 %) |
| Other polymers (%) | < 1 %: PE-C, PVC, NBR, PC, polylactide acid, polycaprolactone, EVA | < 1 %: PVC, NBR, PA, polylactide acid, polycaprolactone, EVA | Acrylates/PUR/varnish (5.6 %), PE (3.9 %), CMC (1.4 %) |

3.4. Environmental and spatial variables

Spearman correlation was conducted to assess the relationship between spatial and environmental variables with total MP concentration, MP particles, and elongated MPs individually. For most variables, there was no relationship revealed. However, significant positive correlations were found between total MP concentrations and concentrations of natural particles, such as chitin ($r_s = 0.71$, $p = 0.001$) and natural polyamides ($r_s = 0.57$, $p = 0.01$). This trend was also found when examining MP particles (chitin: $r_s = 0.72$, $p = 0.001$; natural polyamides: $r_s = 0.56$, $p = 0.02$) and elongated MPs individually (chitin only: $r_s = 0.68$, $p = 0.003$). Further, a positive correlation between MP and quartz particle concentrations was observed across total MPs ($r_s = 0.56$, $p = 0.02$), MP particles ($r_s = 0.55$, $p = 0.02$), and elongated MPs ($r_s = 0.60$, $p = 0.01$; Table S2). These results possibly indicate aggregate formation of MPs with these natural particles or similar transport and dispersal mechanisms.

4. Discussion

Our study provides new data on MP pollution in the Southern Ocean off Antarctica by analyzing MPs down to 11 μm in size. Further, the Weddell Sea is particularly remote and an under-investigated Antarctic region regarding MP pollution, being hard to access due to a perennial sea ice cover and harsh weather conditions.

Because MP abundance is expected to increase with decreasing size, and because smaller MPs may pose greater risks to marine biota due to increased bioavailability at all levels of the food chain, the study of small MPs in the marine environment is of particular importance. The magnitude of the MP pollution problem in the Southern Ocean is probably vastly underestimated because most studies investigating MPs in water samples south of the Antarctic polar front have focused on collecting MPs >300 μm .

4.1. MP concentrations, distribution patterns and possible pathways

Despite the remote sampling region, MPs were detected in all samples, underscoring both the prevalence and the ubiquity of this environmental contaminant. Particular high estimated MP concentrations were detected in the two surface water samples collected in the offshore region of the Weddell Sea (Sample 1 and 2) located north of the 1000-m isobath marking the continental slope and the approximate path of the ASC with total MP concentrations of 267.2 MPs m^{-3} and 259.2 MPs m^{-3} respectively. As these are the first two samples collected, there could be some concern about sample contamination from MPs attached to the sampling device, yet our meticulous QA/QC protocols significantly reduce this risk. A notable drop in MP concentration after the first sampling procedure, the flushing of particles during rinsing/priming and the sampling and filtration process itself, followed by an additional priming/rinsing procedure before Sample 2 was taken, should have resulted in a notable drop in MP concentration in Sample 2 if contamination derived from particles adhering to the sampling device. Nevertheless, Sample 2 retained high MP levels, with even higher concentrations of specific polymers such as PP and PEST compared to Sample 1 (Fig. 1). This is corroborated by the subsequent abrupt decline in MP concentration as well as polymer diversity in the nearshore samples, indicating a true environmental pattern rather than a sampling artefact.

Notably, for Sample 2, only 0.27 m^3 of surface water was collected due to technical issues with the sampling equipment. This volume is less than the recommended minimum of 0.5 m^3 for environmental MP studies (Koelmans et al., 2019; Lofty et al., 2023). Sampling larger volumes is crucial for accurately representing MP distribution in the environment, as smaller volumes might not provide an accurate representation due to the heterogeneous distribution of MPs and possibly lead to over or underestimation of the true MP concentration. Additionally, with smaller sample volumes, potential sample contamination can disproportionately impact the total microplastic count (Cowger et al., 2020; Hidalgo-Ruz et al., 2012). However, assuming that the estimated

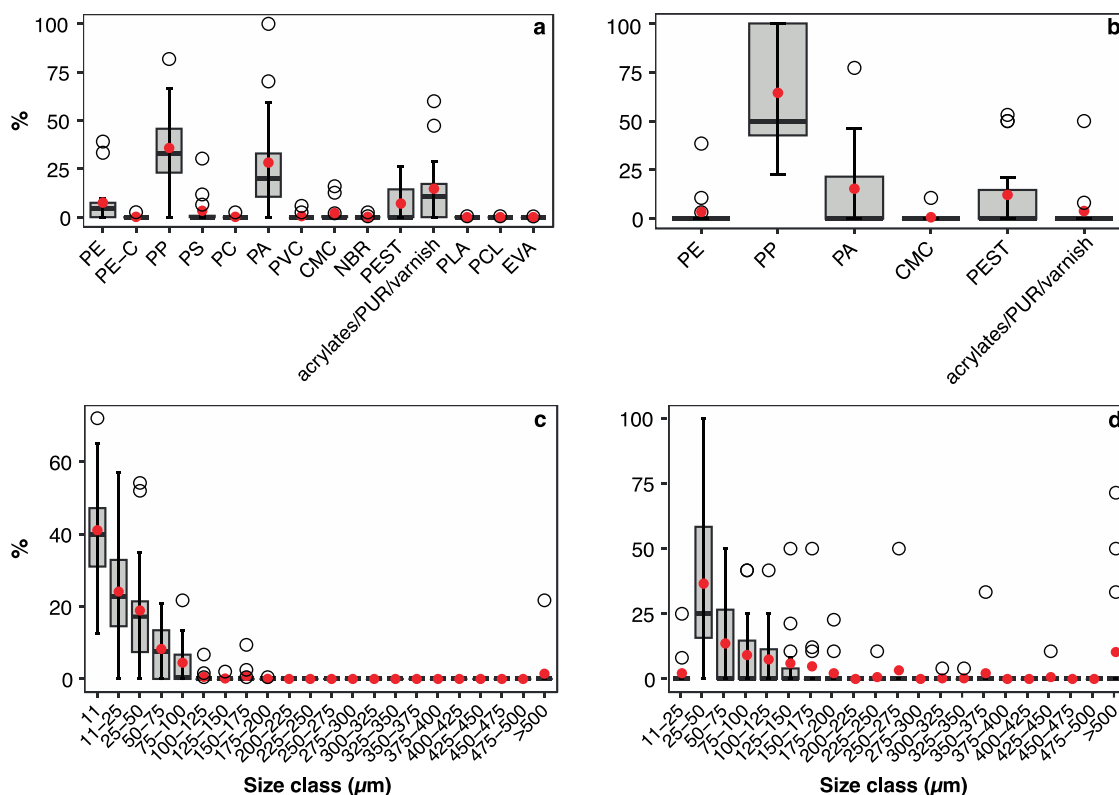


Fig. 2. Box and whisker plots illustrating the percentage (%) shares of identified (a) microplastic (MP) particles and (b) elongated MPs across assigned polymer types, as well as size classes for (c) all identified microplastic particles and (d) elongated microplastic particles in surface water samples. Only samples containing MP particles or elongated MPs are included. The boundary of the box closest to zero indicates the 25th percentile, the line within the box marks the median, and the boundary of the box farthest from zero indicates the 75th percentile. Whiskers (error bars) above and below the box represent the 90th and 10th percentiles. Red dots indicate the mean values and black circles the outliers. Polymer abbreviations are as follows: PE: polyethylene; PE-C: polyethylene-chlorinated; PP: polypropylene; PS: polystyrene; PC: polycarbonate; PA: polyamide; PVC: polyvinylchloride; NBR: nitrile rubber; CMC: chemically modified cellulose; PEST: polyester; acrylates/PUR/varnish: acrylates/polyurethane/varnish/lacquer; PLA: polylactide acid; PCL: polycaprolactone; EVA: ethylene vinyl acetate.

MP concentrations for both Sample 1 and Sample 2 are reasonable, these concentrations are exceptionally high compared to other studies in the Southern Ocean (see Table 2), as well as compared to the other samples collected in the nearshore region in the present study (Fig. 1). The considerable difference in MP concentrations between samples collected offshore and those taken over the continental shelf could be attributed to several factors.

Firstly, the southern Weddell Sea is mostly influenced by the ASC. With a major part of this current flowing westward along the continental shelf break, it may act as a barrier segregating higher microplastic loads in offshore waters from lower concentrations on the shelf by mitigating the mixing between shelf and offshore waters (Thompson et al., 2018). In the southern Weddell Sea, the continental shelf is notably wider than in most other Antarctic regions primarily leading the ASC away from the coastline, yet, some branches of the ASC are still flowing southwards across the continental shelf toward the Filchner-Ronne Ice Shelf with a decreased current velocity (Armitage et al., 2018). These decreased flow velocities in nearshore waters might possibly enhance the sinking of MPs (with high densities, aggregated with natural particulate matter or MPs affected by biofouling). The northerly offshore region might be further influenced by the Weddell Gyre, with the ASC in the southern Weddell Sea being its southern margin. The Weddell Gyre might possibly accumulate MPs, as shown for other ocean gyres in temperate regions and the Arctic (Bryant et al., 2016; Eriksen et al., 2013; Law et al., 2010; Li et al., 2022; Poulain et al., 2018). However, predicting the behavior of surface currents in the study region poses significant challenges and limitations due to highly variable atmospheric influences including katabatic winds and polar cyclones and a strong variability of the ASC, compounded by a deficiency in observational data in the high-latitude Southern Ocean

(Pauthenet et al., 2021; Thompson et al., 2018; Vernet et al., 2019). In addition, the southern margins of the Weddell Gyre and the ASC exhibit complex dynamics of both upwelling (Foster and Carmack, 1976) and downwelling phenomena (Graham et al., 2013; Naveira Garabato et al., 2016; Nøst et al., 2011), which may further influence MP abundance and surface concentrations (Brach et al., 2018).

Another possibility is that the lower MP concentrations found in the samples south of the ASC are influenced by the sea ice conditions and dynamics in the Southern Weddell Sea. The region is characterized by a perennial sea ice cover and coastal polynyas, which are areas of open water or thin newly formed sea ice driven by katabatic winds that advect sea ice away from the coast. The near-shore samples were collected in a coastal polynya west of the Brunt Ice Shelf. It is possible that sea ice may have shielded the surface waters collected in this region from MPs originating further north. Maps of sea ice conditions for each sampling date with the sampling sites marked are provided in the SI (Fig. S7; Grosfeld et al., 2016). Further, it has been shown previously that MPs can accumulate in sea ice (Janssens et al., 2016; Kelly et al., 2020; Peeken et al., 2018), possibly removing MP from the seawater temporarily. New ice formation can be enhanced in coastal polynyas and it is known that particulate matter and microorganisms can be entrapped within freshly formed sea ice, whereby frazil ice crystals scavenge particles from the water column as they rise to the surface (Geilfus et al., 2019; Janssens et al., 2016; Obbard et al., 2014). In coastal polynyas, the newly formed sea ice, together with the entrapped particles, may further be advected away from the coast as fast as it forms. Another suggestion is that MPs accumulate in sea ice as it continues to grow and move through water masses (Peeken et al., 2018). Only considering these samples collected nearshore over the continental shelf, with lower MP

Table 2

Estimates of microplastic (MP) concentrations in surface and subsurface seawater from different regions of the Southern Ocean. For the present study, both total MP concentrations (for the size range 11–>500 μm) and concentrations for MPs > 300 μm only are shown for better comparability with other studies.

| Location | >60°S? | Including elongated MPs? (%) | Water compartment | Mesh size/ detection limit (μm) | Size range (μm) | MP m^{-3} (mean or range) | Dominant polymers | Ref. |
|---|--------------------------|------------------------------------|---------------------|--|--------------------------------------|------------------------------------|-------------------------------|-------------------------------|
| Southern Weddell Sea | Yes | Yes (15 %) | Surface | 11 | 11–>500 | 37.2 \pm 73.8 (0–237.2) | PP, PA | This study |
| | | | Surface | | >300 | 0.07 \pm 0.3 (0–1.1) | | |
| Weddell Sea | Yes | No | Subsurface (11.2 m) | 300 | 130–8700 | 0.01 \pm 0.01 (0–0.04) | PEST, PP, PE | Leistenschneider et al., 2021 |
| | | | Subsurface (11.2 m) | | 277–2994 | 0.04 \pm 0.1 (0–0.47) | Resins, acrylates/PUR/varnish | |
| Antarctic Circumnavigation | Partly | Yes | Surface | 200 | 200–25,000 | 353 ^b | PE, PP ^a | Suaria et al., 2020 |
| Antarctic Circumnavigation | Yes | Yes | Surface | 300 | No MPs | No MPs | No MPs | Kuklinski et al., 2019 |
| East Antarctica | 2 out of 5 samples | No | Surface | 350 | 350–5500 ^a | 0.03–0.09 (only >60°S) | PE, PP ^a | Isobe et al., 2017 |
| Ross Sea | Yes | Yes (13 %) | Subsurface (5 m) | 60 | >60 | 0.17 \pm 0.34 (0.003–1.18) | PE, PP, PEST | Cincinelli et al., 2017 |
| Ross Sea & East Antarctica | Yes | Yes (>90 %) | Surface | 330 | 180–4970 | 0.10 \pm 0.14 (0.006–0.44) | PEST | S. Zhang et al., 2022 |
| | | | Subsurface (8 m) | | 140–4990 | 1.66 \pm 1.20 (0.13–4.41) | PP, PEST, PE | |
| West Antarctic Peninsula | yes | No (including lines > microfibers) | Surface | 330 | 500–75,000 | 0.008 (755–3524 ^b) | PUR, PA | Lacerda et al., 2019 |
| Scotia Sea & Antarctic Peninsula | Yes | Yes (57 %) | Surface | 300 | 150–>10,000 | 0.013 \pm 0.005 | PE, synthetic resins | Jones-Williams et al., 2020 |
| Scotia Sea & Antarctic Peninsula ^a | Partly, starting at 40°S | Yes (30 %) | Subsurface (3 m) | 100 | av. surface area: 0.08 mm^2 | 0.56–0.43 | PET/PEST, PA | Pakhomova et al., 2022 |

^a Including samples collected north of the polar front.

^b Concentrations of plastic items given in items km^{-3} .

concentrations, still a high variability is noticeable. The varying total MP concentrations ranging from 0.47 to 56.13 MPs m^{-3} highlight further challenges caused by particle transport and dispersal by ocean currents and temporal variability when examining marine MP.

The sample collected in the crack between the Brunt Ice Shelf (Sample 17) and the freshly calved Iceberg A74, displayed an estimated MP concentration of 19.3 MPs m^{-3} being not significantly lower than the MP concentrations of Sample 16, taken in front of Iceberg A74, and within the range of concentrations found in other samples collected in the nearshore region. This observation suggests that the surface water collected in the crack was not pristine or freshly exposed. Instead, an influx and mixing with the surrounding water masses, leading to the redistribution of MPs is likely.

Overall, we found exceptionally high MP concentrations compared to previous studies in the Southern Ocean. This result is mainly attributed to small MPs, ranging from 11 μm – 300 μm in size. However, if only MPs > 300 μm are considered, the MP size targeted by the mesh size used in most other studies, the concentration decreases significantly to 0.07 MPs m^{-3} (Table 1). This concentration of larger MPs is in the same order of magnitude as previously reported for surface water samples from the Weddell Sea, East Antarctica and the Scotia Sea and the Antarctic Peninsula (Isobe et al., 2017; Jones-Williams et al., 2020; Leistenschneider et al., 2021), confirming the validity of our sampling approach. However, S. Zhang et al. (2022) reported MP concentrations one order of magnitude higher in East Antarctica and the Ross Sea, which is comparable to concentrations found by Cincinelli et al. (2017) in the Ross Sea and by Pakhomova et al. (2022) in the Scotia Sea and Antarctic Peninsula region. The latter two studies used a lower size limit of 60 μm and 100 μm , respectively, which explains the higher MP concentrations compared to most studies including only larger MPs (Table 2).

4.2. Morphology of MPs

It was found that small MPs, especially those below 50 μm , are dominant in both individual samples and the total quantity. The predominance of smaller-sized MPs aligns with global trends indicating higher abundance of smaller microplastic particles in the environment (Abel et al., 2021; Barrows et al., 2017; Cabernard et al., 2018; Covernton et al., 2019; Kang et al., 2015; Lorenz et al., 2019; Pabortsava and Lampitt, 2020; Peeken et al., 2018), due to fragmentation processes. Considering long-range transport, from easterly regions via the ASC or north-south transport from regions north of the Polar front as suggested by Isobe et al. (2017) as a mechanism for the delivery of MPs to our sampling area, a prolonged exposure to weathering and fragmentation due to e.g. UV radiation and mechanical abrasion will enhance fragmentation into smaller and smaller MPs. The same would be the case if particles released from local sources get entrapped in the region south of the ACC for an extended period as suggested previously (Isobe et al., 2017; Lacerda et al., 2019; Mountford and Maqueda, 2021). Strong UV radiation in Antarctica, as well as the harsh weather conditions and possible ice interactions, including physical abrasion and possibly freezing and thawing cycles, could cause additional mechanical stress on plastic debris and enhance the fragmentation processes in the region. The prevalence of small MPs combined with possibly enhanced fragmentation processes of MP in marine surface waters south of the polar front highlights the need of including small MPs in future studies to provide a more comprehensive insight into the problem of MP pollution in the Southern Ocean and possible ecological implications, and to avoid underestimation.

Even though the distribution patterns of MP particles and elongated MPs were similar within the study area, we found a prevalence of MP particles in our surface water samples contributing to 85 % of all MPs

detected. This is in accordance with the shape proportions found in the Ross Sea (Cincinelli et al., 2017) and suggests a primary contribution of fragmented MPs, potentially from the abrasion and breakdown of larger plastic debris. Interestingly, other MP studies in the Southern Ocean, which included elongated MPs/fibers in their analyses, found that this shape category contributed to much higher proportions (Table 2). In the surface waters of the Ross Sea and off East Antarctica 90 % of all MPs detected were fibers (S. Zhang et al., 2022), while in the regions of the Scotia Sea and the Antarctic Peninsula between 30 % and 57 % of all MPs were fibers (Buckingham et al., 2022; Jones-Williams et al., 2020; Pakhomova et al., 2022). Fibers often originate from textiles, fishing gear, and other fabric materials. Their presence in high proportions could be linked to the higher local human activities (research, tourism, fishing; Aves et al., 2022; Cincinelli et al., 2017; Munari et al., 2017) in these regions compared to the southern Weddell Sea (Leihy et al., 2020; McCarthy et al., 2022).

4.3. Polymer composition and potential MP sources

Not only the variability in MP concentration but also in polymer diversity and types across different samples underscores the complex nature of MP pollution in the southern Weddell Sea, indicating a range of pollution sources and transport pathways. Samples with higher polymer richness (n_{pol}) could possibly be receiving inputs from more different sources, indicating a confluence of different activities contributing to microplastic pollution. Conversely, samples with lower polymer richness, as sampled in the nearshore region, could reflect more isolated or specific sources of microplastic contamination (Li et al., 2021).

Regarding the polymer types found in our samples, PP and PA emerged as the predominant polymer among both shape categories, with PP being found in all samples. Both polymer types are used in a wide range of applications and are among the most commonly found MPs in the marine environment worldwide (Erni-Cassola et al., 2019; GESAMP, 2016). Thus, long-range transport from distant northerly sources via ocean currents and winds might be possible (Chen et al., 2023; Cunningham et al., 2022; Fraser et al., 2016; Waller et al., 2017). Yet, local sources in the Southern Ocean south of 60°S are also likely. Both, PP and particularly PA are commonly used in fishing gear (Deshpande et al., 2020). Although, there are no fishery activities reported for our study region (CCAMLR Statistical Subarea 48.5) MPs originating from these sources might be transported to the southern Weddell Sea from adjacent areas, including easterly areas (CCAMLR Statistical Subarea 48.6; CCAMLR, 2024) from where MPs might be transported with the ASC. Further, these polymers are found in a wide range of other applications and might possibly originate from equipment, construction material such as insulations, pipes etc., fabrics at local research stations and or shipping including research and tourism. Same is the case for other polymer types found that are less prevalent, such as PEST, PE and acrylates/PUR/varnish, which can possibly originate from similar local sources and could further include marine coatings and paints (Lacerda et al., 2019; Leistenschneider et al., 2021).

Previous studies showed that PP and PA are among the most prevalent MPs in surface and subsurface waters of different regions in the Southern Ocean, yet PEST and PE appeared to be even more prevalent in most studies (Table 2). Also, in our previous study in the Weddell Sea, where MPs >300 μm were sampled mostly in lower latitudes and partly further east compared to this study, PEST and PE were identified to dominate (Leistenschneider et al., 2021; Table 2). This could reflect regional differences in the sources and uses of plastic materials. For instance, PEST and PE are prominent in consumer goods and packaging, which could be more prevalent in areas with higher research activity or near established research stations and tourist routes.

Another possibility might be that due to different fragmentation processes, PA and PP are particularly found in the smaller MP size classes which were not considered in previous studies. For example, in an experiment by Meides et al. (2022), PP pellets subjected to

accelerated weathering by exposure to simulated solar radiation and mechanical stress in water degraded approximately 4 times faster than PE (Menzel et al., 2022). It is important to note that the composition of chemical additives in plastics, such as UV stabilizers, as well as the environmental forces driving MP fragmentation can be complex and affect the process. However, it has been shown for PP that the addition of stabilizers only prevented degradation for a short period of time, after which PP with and without stabilizers had comparable properties and sizes (Meides et al., 2022).

Particles identified as rubber type 3 (RT3), acrylamides and ship paint from the RV *Polarstern* were excluded from our study due to indications of inaccurate spectral matching or potential misidentifications with lipids/stearates after manual spectral evaluation of 100 randomly selected spectra (Fig. S5). In particular, the one sample that could not be sufficiently purified from the white residues (Sample 3), even after the inclusion of the second density separation step, supports this. Here, a particularly high number of these polymer types was identified, what could be due to lipids derived from diatoms, for example. It should be noted, however, that in our previous study investigating MPs >300 μm in the surface waters of the Weddell Sea, a significant number of ship paint particles were detected from our sampling vessel, the RV *Polarstern* (Leistenschneider et al., 2021). Yet, the identification of these particles using FTIR spectroscopy alone was not possible due to poor quality spectra, requiring a complementary approach combining both FTIR and micro X-ray fluorescence spectroscopy ($\mu\text{-XRF}$) for accurate identification. In our current study, which aims to detect synthetic particles as small as 11 μm , the lack of a $\mu\text{-XRF}$ system with the required lower detection limit, coupled with time constraints, made this combined approach unfeasible. However, given the previously demonstrated importance of this type of MP as a source of both sample and environmental contamination, their brief mention here is essential.

4.4. Co-occurrence of MPs and natural particles

Our findings indicate that concentrations of MPs positively correlate with concentrations of natural particles identified as chitin, natural polyamides suggesting keratinous particles, and quartz or SiO_2 , which may derive from diatom frustules. This suggests a potential association between MPs and these natural particles, potentially due to similar environmental transport mechanisms or aggregation behaviors.

The densities of diatom frustules ($\rho = 1.1\text{--}1.6 \text{ g/cm}^3$; Hamano et al., 2021; Miklasz and Denny, 2010) or pure quartz ($\rho = 2.65 \text{ g/cm}^3$; Lide, 2004), keratinous structures ($\rho \sim 1.2\text{--}1.3 \text{ g/cm}^3$; Elden, 1968; Mason, 1963), and chitin ($\rho \sim 1.4 \text{ g/cm}^3$; Carlström, 1957) suggest that these particles would typically sink. However, the density of materials originating from natural structures such as e.g., diatom frustules, exoskeletons, fur, and feathers can vary depending on their composition (e.g. including proteins and sugars; Hamano et al., 2021) and structure, which may include pores and other structures entrapping air (Hamano et al., 2021; Sullivan et al., 2017), and possibly also due to attached organic tissue or aggregation with other floating particles.

Interestingly, the MP polymer types showing the strongest correlation with the natural particles were PA ($\rho = 1.01\text{--}1.15 \text{ g/cm}^3$; Wypych, 2012), CMC ($\rho = 1.5\text{--}1.6 \text{ g/cm}^3$; Wypych, 2012), and PEST ($\rho = 1.38\text{--}1.41 \text{ g/cm}^3$; Wypych, 2012) for chitin, PA and CMC for natural polyamides, and PA and PE ($\rho = 0.91\text{--}0.96 \text{ g/cm}^3$; Wypych, 2012) for quartz/diatom frustules (Table S2). With the exception of PE, these are all synthetic polymers with densities higher than water, similar to the natural particles mentioned. This may explain their simultaneous presence and their analogous behavior and/or transport mechanisms. Despite their density, these MPs were found at the water surface, which is a common observation in MP studies (Erni-Cassola et al., 2019). It is possible that these particles are held at the water surface by the surface water tension (Song et al., 2014) or by vertical mixing and upwelling. In particular, smaller high-density MPs, being denser than water, may be kept afloat or suspended by turbulent mixing, which may counteract

their natural tendency to sink (Shamskhany and Karimpour, 2022). Regarding the correlation of PE and quartz/SiO₂ concentrations, buoyancy mechanisms of living diatoms, such as lipid content regulation (Zhang et al., 2023) could explain the co-occurrence of buoyant PE with quartz particles, possibly derived from diatom frustules. The consistent correlations found across the different MP shapes with the natural particles may indicate that the shapes do not significantly alter the transport mechanisms and association with these natural particles. That the transport mechanisms of the different MP shapes, MP particles and elongated MPs, may be similar is also suggested by the similar distribution pattern within the sampling area (Fig. 1).

5. Conclusion

Marine MP pollution is already known to be widespread, including in the Southern Ocean south of the polar front, despite this region being considered pristine and remote. However, the extent of MP pollution in the marine environment off Antarctica is likely to be greatly underestimated due to sampling and analytical methods that do not include small MPs. Our results, which included MPs as small as 11 µm, showed particularly high concentrations of MPs in surface water samples from one of the world's most remote regions, the southern Weddell Sea, which were dominated by the smallest MPs. This highlights the urgent need to focus future research on small MPs to gain a comprehensive understanding of microplastic pollution and the potential impacts and risks to this unique and sensitive environment. Particularly as studies suggest that the smaller the plastic particles, the more toxic they are to marine biota (Ferreira et al., 2019; Jeong et al., 2016; Sun et al., 2019). This includes Antarctic krill, a keystone species in the Southern Ocean, which has been found to ingest MPs (Wilkie Johnston et al., 2023; Zhu et al., 2023), although a recent study highlights the importance of further investigation to estimate the real extend of this problem (Primpke et al., 2024). Nevertheless, the development and behavior of krill have been found to be affected by the uptake of nanoplastics (Bergami et al., 2020; Rowlands et al., 2021) which have been shown to penetrate tissues and cross the blood-brain barrier in other aquatic biota (Al-Sid-Cheikh et al., 2018; Mattsson et al., 2017; Sökmen et al., 2020; von Moos et al., 2012). However, methods for investigating nanoplastics in the environment are currently still evolving, with challenges and limitations in separation, identification, and quantification (Moon et al., 2024).

In our study, the presence of MPs in all samples shows that microplastic pollution is ubiquitous even in the Weddell Sea, while the variability of MP concentrations and polymer types indicates the influence of complex transport pathways and different pollution sources, underscoring the need for ongoing research and continuous monitoring.

In light of our findings, it is imperative that future research adopts a multidisciplinary approach that investigates the complex interactions between microplastic pollution and various environmental dynamics. This includes investigating/modelling the interactions with ocean currents, eddies and turbulence, flow velocities and atmospheric forces that may affect the horizontal and vertical transport and distribution of MPs. In addition, aggregation and fragmentation processes in the environment and the dynamics of interactions with sea ice are important factors that require further study. By addressing these issues, future studies could provide a more holistic understanding of MP pollution in the Southern Ocean, thereby helping to unravel the intricacies of microplastic distribution, sources and ecological impacts in this pristine region, and enhancing our ability to formulate effective mitigation strategies and conservation efforts for these pristine environments.

Funding

This study was supported by the Alfred-Wegener-Institut Helmholtz-Zentrum für Polar- und Meeresforschung (AWI, Germany; Grant No. AWI_PS124 10) the Ricola Foundation (Switzerland) and the Freiwillige Akademische Gesellschaft Basel (FAG, Switzerland). G.G. and F.W. were

supported within the framework of JPI Oceans by the German Federal Ministry of Education and Research (Project FACTS - Fluxes and Fate of Microplastics in Northern European Waters; BMBF grant 03F0849A). S. P. was supported by funding from the European Union's Horizon 2020 Coordination and Support Action programme under Grant agreement 101003805 (EUROqCHARM). This output reflects only the author's view and the European Union cannot be held responsible for any use that may be made of the information contained therein.

CRedit authorship contribution statement

Clara Leistschneider: Writing – review & editing, Writing – original draft, Visualization, Methodology, Investigation, Formal analysis, Data curation. **Fangzhu Wu:** Writing – review & editing, Investigation. **Sebastian Primpke:** Writing – review & editing, Formal analysis. **Gunnar Gerdts:** Writing – review & editing, Supervision, Methodology, Conceptualization. **Patricia Burkhardt-Holm:** Writing – review & editing, Supervision, Funding acquisition, Conceptualization.

Declaration of competing interest

The authors declare that they have no known competing financial interests or personal relationships that could have appeared to influence the work reported in this paper.

Data availability

Data will be made available on request.

Acknowledgments

We are grateful for the logistical and technical support during expedition PS124 from the entire crew of RV *Polarstern*: Alfred-Wegener-Institut Helmholtz-Zentrum für Polar- und Meeresforschung (2017). Polar Research and Supply Vessel POLARSTERN Operated by the Alfred-Wegener-Institute. Journal of large-scale research facilities, 3, A119. <https://doi.org/10.17815/jlsrf-3-163>. Likewise, we are grateful for the support of the workshop staff at AWI Helgoland with adjustments and initial tests of the sampling and filtration systems, and the crew of RV *Uthörn*, as well as Susann Henkel (AWI Bremerhaven) for assistance in shipping the samples to AWI Helgoland. We thank Nicole Seiler-Kurth and Heidi Schiffer (MGU, University of Basel) for their great support during the preparation of the expedition and freight, and Hannah Jebens (AWI Helgoland) for laboratory support. Further, we would like to thank Ralph Timmermann (AWI Bremerhaven), for providing valuable information on the circulation dynamics in the sampling region and Serena Abel (MGU, University of Basel) for proofreading.

Appendix A. Supplementary data

Supplementary data to this article can be found online at <https://doi.org/10.1016/j.scitotenv.2024.172124>.

References

- Abel, S.M., Primpke, S., Int-Veen, I., Brandt, A., Gerdts, G., 2021. Systematic identification of microplastics in abyssal and hadal sediments of the Kuril Kamchatka trench. *Environ. Pollut.* 269, 116095 <https://doi.org/10.1016/j.envpol.2020.116095>.
- Abel, S.M., Primpke, S., Wu, F., Brandt, A., Gerdts, G., 2022. Human footprints at hadal depths: interlayer and intralayer comparison of sediment cores from the Kuril Kamchatka trench. *Sci. Total Environ.* 838, 156035 <https://doi.org/10.1016/j.scitotenv.2022.156035>.
- Al-Azzawi, M.S.M., Kefer, S., Weißer, J., Reichel, J., Schwaller, C., Glas, K., Knoop, O., Drewes, J.E., 2020. Validation of sample preparation methods for microplastic analysis in wastewater matrices—reproducibility and standardization. *Water* 12, 2445. <https://doi.org/10.3390/w12092445>.
- Al-Sid-Cheikh, M., Rowland, S.J., Stevenson, K., Rouleau, C., Henry, T.B., Thompson, R.C., 2018. Uptake, whole-body distribution, and depuration of Nanoplastics by the

- scallop *Pecten maximus* at environmentally realistic concentrations. *Environ. Sci. Technol.* 52, 14480–14486. <https://doi.org/10.1021/acs.est.8b05266>.
- Armitage, T.W.K., Kwok, R., Thompson, A.F., Cunningham, G., 2018. Dynamic topography and sea level anomalies of the Southern Ocean: variability and teleconnections. *J. Geophys. Res.: Oceans* 123, 613–630. <https://doi.org/10.1002/2017JC013534>.
- Arthur, C., Baker, J., Bamford, H.A., 2009. Proceedings of the International Research Workshop on the Occurrence, Effects, and Fate of Microplastic Marine Debris, September 9–11, 2008. NOAA Technical Memorandum NOS-OR&R-30. University of Washington Tacoma, Tacoma, WA, USA.
- Aves, A.R., Revell, L.E., Gaw, S., Ruffell, H., Schuddeboom, A., Wotherspoon, N.E., LaRue, M., McDonald, A.J., 2022. First evidence of microplastics in Antarctic snow. *Cryosphere* 16, 2127–2145. <https://doi.org/10.5194/tc-16-2127-2022>.
- Barrows, A.P.W., Neumann, C., Berger, M., Shaw, S., 2017. Grab vs. neuston tow net: a microplastic sampling performance comparison and possible advances in the field. *Anal. Methods* 9, 1446–1453. <https://doi.org/10.1039/C6AY02387H>.
- Batel, A., Linti, F., Scherer, M., Erdinger, L., Braunbeck, T., 2016. Transfer of benzo[*a*]pyrene from microplastics to *Artemia* nauplii and further to zebrafish via a trophic food web experiment: CYP1A induction and visual tracking of persistent organic pollutants. *Environ. Toxicol. Chem.* 35, 1656–1666. doi:<https://doi.org/10.1002/et.c.3361>.
- Bergami, E., Manno, C., Cappello, S., Vannuccini, M.L., Corsi, I., 2020. Nanoplastics affect moulting and faecal pellet sinking in Antarctic krill (*Euphausia superba*) juveniles. *Environ. Int.* 143, 105999. <https://doi.org/10.1016/j.envint.2020.105999>.
- Bergami, E., Ferrari, E., Löder, M.G.J., Birarda, G., Laforsch, C., Vaccari, L., Corsi, I., 2023. Textile microfibers in wild Antarctic whelk *Neobuccinum eatoni* (Smith, 1875) from Terra Nova Bay (Ross Sea, Antarctica). *Environ. Res.* 216, 114487. <https://doi.org/10.1016/j.envres.2022.114487>.
- Bergmann, M., Tekman, M.B., Gutow, L., 2017. Sea change for plastic pollution. *Nature* 544, 297. <https://doi.org/10.1038/544297a>.
- Brach, L., Deixonne, P., Bernard, M.-F., Durand, E., Desjean, M.-C., Perez, E., van Sebille, E., Ter Halle, A., 2018. Anticyclonic eddies increase accumulation of microplastic in the North Atlantic subtropical gyre. *Mar. Pollut. Bull.* 126, 191–196. <https://doi.org/10.1016/j.marpolbul.2017.10.077>.
- Bryant, J.A., Clemente, T.M., Viviani, D.A., Fong, A.A., Thomas, K.A., Kemp, P., Karl, D.M., White, A.E., DeLong, E.F., 2016. Diversity and activity of communities inhabiting plastic debris in the North Pacific Gyre. *mSystems* 11. <https://doi.org/10.1128/mSystems.00024-16>.
- Buckingham, J.W., Manno, C., Waluda, C.M., Waller, C.L., 2022. A record of microplastic in the marine nearshore waters of South Georgia. *Environ. Pollut.* 306, 119379. <https://doi.org/10.1016/j.envpol.2022.119379>.
- Cabernard, L., Roscher, L., Lorenz, C., Gerdt, G., Primpke, S., 2018. Comparison of Raman and Fourier transform infrared spectroscopy for the quantification of microplastics in the aquatic environment. *Environ. Sci. Technol.* 52, 13279–13288. <https://doi.org/10.1021/acs.est.8b03438>.
- Cao, Y., Zhao, M., Ma, X., Song, Y., Zuo, S., Li, H., Deng, W., 2021. A critical review on the interactions of microplastics with heavy metals: mechanism and their combined effect on organisms and humans. *Sci. Total Environ.* 788, 147620. <https://doi.org/10.1016/j.scitotenv.2021.147620>.
- Carlström, D., 1957. THE CRYSTAL STRUCTURE OF α -CHITIN (POLY-N-ACETYL-D-GLUCOSAMINE). *J. Biophys. Biochem. Cytol.* 3, 669–683. <https://doi.org/10.1083/jcb.3.5.669>.
- Chen, Q., Shi, G., Revell, L.E., Zhang, J., Zuo, C., Wang, D., Le Ru, E.C., Wu, G., Mitran, D.M., 2023. Long-range atmospheric transport of microplastics across the southern hemisphere. *Nat. Commun.* 14, 7898. <https://doi.org/10.1038/s41467-023-43695-0>.
- Cincinelli, A., Scopetani, C., Chelazzi, D., Lombardini, E., Martellini, T., Katsoyiannis, A., Fossi, M.C., Corsolini, S., 2017. Microplastic in the surface waters of the Ross Sea (Antarctica): occurrence, distribution and characterization by FTIR. *Chemosphere* 175, 391–400. <https://doi.org/10.1016/j.chemosphere.2017.02.024>.
- Commission for the Conservation of Antarctic Marine Living Resources (CCAMLR), 2024. Fishery Reports. Available at: <https://fisheryreports.ccamlr.org/>. [Accessed: 01.03.2024].
- Covernton, G.A., Pearce, C.M., Gurney-Smith, H.J., Chastain, S.G., Ross, P.S., Dower, J. F., Dudas, S.E., 2019. Size and shape matter: a preliminary analysis of microplastic sampling technique in seawater studies with implications for ecological risk assessment. *Sci. Total Environ.* 667, 124–132. <https://doi.org/10.1016/j.scitotenv.2019.02.346>.
- Cowger, W., Booth, A.M., Hamilton, B.M., Thaysen, C., Primpke, S., Munno, K., Lusher, A.L., Dehaut, A., Vaz, V.P., Libouiro, M., Devriese, L.I., Hermabessiere, L., Rochman, C., Athey, S.N., Lynch, J.M., Frond, H.D., Gray, A., Jones, O.A.H., Brander, S., Steele, C., Moore, S., Sanchez, A., Nel, H., 2020. Reporting guidelines to increase the reproducibility and comparability of research on microplastics. *Appl. Spectrosc.* 74, 1066–1077. <https://doi.org/10.1364/AS.74.001066>.
- Cunningham, E.M., Ehlers, S.M., Dick, J.T.A., Sigwart, J.D., Linse, K., Dick, J.J., Kiriakoulakis, K., 2020. High abundances of microplastic pollution in Deep-Sea sediments: evidence from Antarctica and the Southern Ocean. *Environ. Sci. Technol.* 54, 13661–13671. <https://doi.org/10.1021/acs.est.0c03441>.
- Cunningham, E.M., Rico Seijo, N., Altieri, K.E., Audh, R.R., Burger, J.M., Bornman, T.G., Fawcett, S., Gwinnett, C.M.B., Osborne, A.O., Woodall, L.C., 2022. The transport and fate of microplastic fibres in the Antarctic: the role of multiple global processes. *Front. Mar. Sci.* 9. <https://doi.org/10.3389/fmars.2022.1056081>.
- Deshpande, P.C., Philis, G., Brattebø, H., Fet, A.M., 2020. Using material flow analysis (MFA) to generate the evidence on plastic waste management from commercial fishing gears in Norway. *Resources, Conservation & Recycling: X* 5, 100024. <https://doi.org/10.1016/j.rcrx.2019.100024>.
- Dorschel, B., Hehemann, L., Viquerat, S., Warnke, F., Dretter, S., Tenberge, Y.S., Accetella, D., An, L., Barrios, F., Bazhenova, E.A., Black, J., Bohoyo, F., Davey, C., Santis, L. de, Dotti, C.E., Fremard, A.C., Fretwell, P.T., Gales, J.A., Gao, J., Gasperini, L., Greenbaum, J.S., Jencks, J.H., Hogan, K.A., Hong, J.K., Jakobsen, M., Jensen, L., Kool, J., Larin, S., Larter, R.D., Leitchenkov, G.L., Loubrieu, B., Mackay, K., Mayer, L., Millan, R., Morlighem, M., Navidad, F., Nitsche, F.-O., Nogé, Y., Pertuisot, C., Post, A.L., Pritchard, H.D., Purser, A., Rebesco, M., Rignot, E., Roberts, J.L., Rovere, M., Ryzhov, I., Sauli, C., Schmitt, T., Silvano, A., Smith, J.E., Snaith, H., Tate, A.J., Tinto, K., Vandenbossche, P., Weatherall, P., Wintersteller, P., Yang, C., Zhang, T., Arndt, J.E., 2022. The International Bathymetric Chart of the Southern Ocean Version 2 (IBCSO v2). <https://doi.org/10.1594/PANGAEA.937574>.
- Elden, H.R., 1968. Physical properties of collagen fibers. In: Hall, D.A. (Ed.), *International Review of Connective Tissue Research*. Elsevier, pp. 283–348. <https://doi.org/10.1016/B978-1-4831-6754-1.50013-3>.
- Eriksen, M., Maximenko, N., Thiel, M., Cummins, A., Lattin, G., Wilson, S., Hafner, J., Zellers, A., Rifman, S., 2013. Plastic pollution in the South Pacific subtropical gyre. *Mar. Pollut. Bull.* 68, 71–76. <https://doi.org/10.1016/j.marpolbul.2012.12.021>.
- Erni-Cassola, G., Zadjelovic, V., Gibson, M.I., Christie-Oleza, J.A., 2019. Distribution of plastic polymer types in the marine environment; a meta-analysis. *J. Hazard. Mater.* 369, 691–698. <https://doi.org/10.1016/j.jhazmat.2019.02.067>.
- Evangelou, N., Grythe, H., Klimont, Z., Heyes, C., Eckhardt, S., Lopez-Aparicio, S., Stohl, A., 2020. Atmospheric transport is a major pathway of microplastics to remote regions. *Nat. Commun.* 11, 3381. <https://doi.org/10.1038/s41467-020-17201-9>.
- Ferreira, I., Venâncio, C., Lopes, I., Oliveira, M., 2019. Nanoplastics and marine organisms: what has been studied? *Environ. Toxicol. Pharmacol.* 67, 1–7. <https://doi.org/10.1016/j.etap.2019.01.006>.
- Foster, T.D., Carmack, E.C., 1976. Temperature and salinity structure in the Weddell Sea. *J. Phys. Oceanogr.* 6, 36–44. [https://doi.org/10.1175/1520-0485\(1976\)006<0036:TASSIT>2.0.CO;2](https://doi.org/10.1175/1520-0485(1976)006<0036:TASSIT>2.0.CO;2).
- Fragão, J., Bessa, F., Otero, V., Barbosa, A., Sobral, P., Waluda, C.M., Guímaro, H.R., Xavier, J.C., 2020. Microplastics and other anthropogenic particles in Antarctica: using penguins as biological samplers. *Sci. Total Environ.* 788, 147698. <https://doi.org/10.1016/j.scitotenv.2021.147698>.
- Fraser, C.I., Kay, G.M., Plessis, M. du, Ryan, P.G., 2016. Breaking down the barrier: dispersal across the Antarctic polar front. *Ecography* 40, 235–237. <https://doi.org/10.1111/ecog.02449>.
- Fraser, C.I., Morrison, A.K., Hogg, A.M., Macaya, E.C., van Sebille, E., Ryan, P.G., Padovan, A., Jack, C., Valdivia, N., Waters, J.M., 2018. Antarctica's ecological isolation will be broken by storm-driven dispersal and warming. *Nat. Clim. Chang.* 8, 704–708. <https://doi.org/10.1038/s41558-018-0209-7>.
- García-Garin, O., García-Cuevas, I., Drago, M., Rita, D., Parga, M., Gazo, M., Cardona, L., 2020. No evidence of microplastics in Antarctic fur seal scats from a hotspot of human activity in Western Antarctica. *Sci. Total Environ.* 737, 140210. <https://doi.org/10.1016/j.scitotenv.2020.140210>.
- Geilfus, N.-X., Munson, K.M., Sousa, J., Germanov, Y., Bhugalo, S., Babb, D., Wang, F., 2019. Distribution and impacts of microplastic incorporation within sea ice. *Mar. Pollut. Bull.* 145, 463–473. <https://doi.org/10.1016/j.marpolbul.2019.06.029>.
- GESAMP, Joint Group of Experts on the Scientific Aspects of Marine Environmental Protection, 2016. Sources, fate and effects of microplastics in the marine environment: part two of a global assessment Reports and Studies GESAMP No. 93, p. 16. International Maritime Organization.
- González-Pleiter, M., Edo, C., Velázquez, D., Casero-Chamorro, M.C., Leganés, F., Quesada, A., Fernández-Piñas, F., Rosal, R., 2020. First detection of microplastics in the freshwater of an Antarctic specially protected area. *Mar. Pollut. Bull.* 161, 111811. <https://doi.org/10.1016/j.marpolbul.2020.111811>.
- González-Pleiter, M., Lacerot, G., Edo, C., Pablo Lozoya, J., Leganés, F., Fernández-Piñas, F., Rosal, R., Teixeira-de-Mello, F., 2021. A pilot study about microplastics and mesoplastics in an Antarctic glacier. *The Cryosphere* 15, 2531–2539. <https://doi.org/10.5194/tc-15-2531-2021>.
- Graham, J.A., Heywood, K.J., Chavanne, C.P., Holland, P.R., 2013. Seasonal variability of water masses and transport on the Antarctic continental shelf and slope in the southeastern Weddell Sea. *J. Geophys. Res.: Oceans* 118, 2201–2214. doi:<https://doi.org/10.1002/jgrc.20174>.
- Grosfeld, K., Treffeisen, R., Asseng, J., Bartsch, A., Bräuer, B., Fritsch, B., Gerdes, R., Hendricks, S., Hiller, W., Heygster, G., Krumpfen, T., Lemke, P., Melsheimer, C., Nicolaus, M., Ricker, R., Weigelt, M., 2016. Online Sea-ice Knowledge and data platform. *Polarforschung* 85. <https://doi.org/10.2312/POLFOR.2016.011>.
- Gündoğdu, S., 2022. Polymer types of microplastic in coastal areas. In: Hashmi, M.Z. (Ed.), *Microplastic Pollution: Environmental Occurrence and Treatment Technologies, Emerging Contaminants and Associated Treatment Technologies*. Springer International Publishing, Cham, pp. 77–88. https://doi.org/10.1007/978-3-030-89220-3_4.
- Gurumoorthi, K., Luis, A.J., 2023. Recent trends on microplastics abundance and risk assessment in coastal Antarctica: regional meta-analysis. *Environ. Pollut.* 324, 121385. <https://doi.org/10.1016/j.envpol.2023.121385>.
- Haas, C., Arndt, S., Peeken, I., Eggert, S. L., & Neudert, M. (2021). Sea ice geophysics and biochemistry. In H. H. Hellmer & M. Holtappels (Eds.), *The Expedition PS124 of the Research Vessel POLARSTERN to the southern Weddell Sea in 2021* (pp. 93–97). *Berichte zur Polar- und Meeresforschung - Reports on polar and marine research*. doi:<https://doi.org/10.48433/BzPM.0755.2021>.
- Hamano, R., Shoumura, S., Takeda, Y., Yamazaki, T., Hirayama, K., Hanada, Y., Mayama, S., Takemura, M., Lin, H.-J., Umemura, K., 2021. Sinking of four species of living diatom cells directly observed by a “tumbled” optical microscope. *Microsc. Microanal.* 27, 1154–1160. <https://doi.org/10.1017/S143197621012150>.
- Hellmer, H.H., Holtappels, M., 2021. The expedition PS124 of the research vessel POLARSTERN to the southern Weddell Sea in 2021. *Berichte zur Polar- und*

- Meeresforschung - Reports on polar and marine research. <https://doi.org/10.48433/BzPM.0755.2021>.
- Hidalgo-Ruz, V., Gutow, L., Thompson, R.C., Thiel, M., 2012. Microplastics in the marine environment: a review of the methods used for identification and quantification. *Environ. Sci. Technol.* 46, 3060–3075. <https://doi.org/10.1021/es2031505>.
- Howell, E.A., Bograd, S.J., Morishige, C., Seki, M.P., Polovina, J.J., 2012. On North Pacific circulation and associated marine debris concentration. *Mar. Pollut. Bull. At-sea Detection of Derelict Fishing Gear* 65, 16–22. <https://doi.org/10.1016/j.marpolbul.2011.04.034>.
- Huneke, W.G.C., Morrison, A.K., Hogg, A.M., 2022. Spatial and Subannual Variability of the Antarctic Slope Current in an Eddyding Ocean–Sea Ice Model. *J. Phys. Oceanogr.* 52, 347–361. doi:<https://doi.org/10.1175/JPO-D-21-0143.1>.
- Huneke, W.G.C., Morrison, A.K., Hogg, A.M.C., 2023. Decoupling of the surface and bottom-intensified Antarctic slope current in regions of dense shelf water export. *Geophys. Res. Lett.* 50, e2023GL104834 <https://doi.org/10.1029/2023GL104834>.
- Isobe, A., Kubo, K., Tamura, Y., Kako, S., Nakashima, E., Fujii, N., 2014. Selective transport of microplastics and mesoplastics by drifting in coastal waters. *Mar. Pollut. Bull.* 89, 324–330. <https://doi.org/10.1016/j.marpolbul.2014.09.041>.
- Isobe, A., Uchiyama-Matsumoto, K., Uchida, K., Tokai, T., 2017. Microplastics in the Southern Ocean. *Mar. Pollut. Bull.* 114, 623–626. <https://doi.org/10.1016/j.marpolbul.2016.09.037>.
- Janssens, J., Meiners, K.M., Tison, J.-L., Dieckmann, G., Delille, B., Lannuzel, D., 2016. Incorporation of iron and organic matter into young Antarctic Sea ice during its initial growth stages. *Elementa: Science of the Anthropocene* 4, 000123. <https://doi.org/10.12952/journal.elementa.000123>.
- Jeong, C.-B., Won, E.-J., Kang, H.-M., Lee, M.-C., Hwang, D.-S., Hwang, U.-K., Zhou, B., Souissi, S., Lee, S.-J., Lee, J.-S., 2016. Microplastic size-dependent toxicity, oxidative stress induction, and p-JNK and p-p38 activation in the Monogonot rotifer (*Brachionus koreanus*). *Environ. Sci. Technol.* 50, 8849–8857. <https://doi.org/10.1021/acs.est.6b01441>.
- Jones-Williams, K., Galloway, T., Cole, M., Stowasser, G., Waluda, C., Manno, C., 2020. Close encounters - microplastic availability to pelagic amphipods in sub-antarctic and antarctic surface waters. *Environ. Int.* 140, 105792 <https://doi.org/10.1016/j.envint.2020.105792>.
- Kang, J.-H., Kwon, O.Y., Lee, K.-W., Song, Y.K., Shim, W.J., 2015. Marine neustonic microplastics around the southeastern coast of Korea. *Mar. Pollut. Bull.* 96, 304–312. <https://doi.org/10.1016/j.marpolbul.2015.04.054>.
- Kelly, A., Lannuzel, D., Rodemann, T., Meiners, K.M., Auman, H.J., 2020. Microplastic contamination in East Antarctic Sea ice. *Mar. Pollut. Bull.* 154, 111130 <https://doi.org/10.1016/j.marpolbul.2020.111130>.
- Koelmans, A.A., Mohamed Nor, N.H., Hermens, E., Kooi, M., Mintenig, S.M., De France, J., 2019. Microplastics in freshwaters and drinking water: critical review and assessment of data quality. *Water Res.* 155, 410–422. <https://doi.org/10.1016/j.watres.2019.02.054>.
- Kögel, T., Bjørøy, Ø., Toto, B., Bienfait, A.M., Sanden, M., 2020. Micro- and nanoplastic toxicity on aquatic life: determining factors. *Sci. Total Environ.* 709, 136050 <https://doi.org/10.1016/j.scitotenv.2019.136050>.
- Kuklinski, P., Wicikowski, L., Koper, M., Grala, T., Leniec-Koper, H., Barasiński, M., Talar, M., Kamiński, I., Kibart, R., Małecki, W., 2019. Offshore surface waters of Antarctica are free of microplastics, as revealed by a circum-Antarctic study. *Mar. Pollut. Bull.* <https://doi.org/10.1016/j.marpolbul.2019.110573>.
- Lacerda, A.L.D.F., Rodrigues, L. dos S., van Sebille, E., Rodrigues, F.L., Ribeiro, L., Secchi, E.R., Kessler, F., Proietti, M.C., 2019. Plastics in sea surface waters around the Antarctic peninsula. *Sci. Rep.* 9 <https://doi.org/10.1038/s41598-019-40311-4>.
- Law, K.L., Morét-Ferguson, S., Maximenko, N.A., Proskurowski, G., Peacock, E.E., Hafner, J., Reddy, C.M., 2010. Plastic accumulation in the North Atlantic subtropical gyre. *Science* 329, 1185–1188. <https://doi.org/10.1126/science.1192321>.
- Leihy, R.L., Coetzee, B.W.T., Morgan, F., Raymond, B., Shaw, J.D., Terauds, A., Bastmeijer, K., Chown, S.L., 2020. Antarctica's wilderness fails to capture continent's biodiversity. *Nature* 583, 567–571. <https://doi.org/10.1038/s41586-020-2506-3>.
- Leistenschneider, C., Burkhardt-Holm, P., Mani, T., Primpke, S., Taubner, H., Gerdts, G., 2021. Microplastics in the Weddell Sea (Antarctica): a forensic approach for discrimination between environmental and vessel-induced microplastics. *Environ. Sci. Technol.* 55, 15900–15911. <https://doi.org/10.1021/acs.est.1c05207>.
- Leistenschneider, C., Le Bohec, C., Eisen, O., Houstin, A., Neff, S., Primpke, S., Zitterbart, D.P., Burkhardt-Holm, P., Gerdts, G., 2022. No evidence of microplastic ingestion in emperor penguin chicks (*Aptenodytes forsteri*) from the Atka Bay colony (Dronning Maud land, Antarctica). *Sci. Total Environ.* 851, 158314 <https://doi.org/10.1016/j.scitotenv.2022.158314>.
- Li, C., Gan, Y., Zhang, C., He, H., Fang, J., Wang, L., Wang, Y., Liu, J., 2021. "Microplastic communities" in different environments: differences, links, and role of diversity index in source analysis. *Water Res.* 188, 116574 <https://doi.org/10.1016/j.watres.2020.116574>.
- Li, J., Gao, F., Zhang, D., Cao, W., Zhao, C., 2022. Zonal distribution characteristics of microplastics in the southern Indian Ocean and the influence of ocean current. *J. Mar. Sci. Eng.* 10, 290. <https://doi.org/10.3390/jmse10020290>.
- Lide, D.R., 2004. *CRC Handbook of Chemistry and Physics*, 85th edition. CRC Press.
- Lofty, J., Ouro, P., Wilson, C.A.M.E., 2023. Microplastics in the riverine environment: Meta-analysis and quality criteria for developing robust field sampling procedures. *Sci. Total Environ.* 863, 160893 <https://doi.org/10.1016/j.scitotenv.2022.160893>.
- Lorenz, C., Roscher, L., Meyer, M.S., Hildebrandt, L., Prume, J., Löder, M.G.J., Primpke, S., Gerdts, G., 2019. Spatial distribution of microplastics in sediments and surface waters of the southern North Sea. *Environ. Pollut.* 252, 1719–1729. <https://doi.org/10.1016/j.envpol.2019.06.093>.
- Mason, P., 1963. Density and structure of alpha-keratin. *Nature* 197, 179–180. <https://doi.org/10.1038/197179a0>.
- Matsuoka, K., Skoglund, A., Roth, G., de Pomereu, J., Griffiths, H., Headland, R., Herried, B., Katsumata, K., Le Brocq, A., Licht, K., Morgan, F., Neff, P.D., Ritz, C., Scheinert, M., Tamura, T., Van de Putte, A., van den Broeke, M., von Deschanden, A., Deschamps-Berger, C., Van Liefferinge, B., Tronstad, S., Melvær, Y., 2021. Quantarctica, an integrated mapping environment for Antarctica, the Southern Ocean, and sub-Antarctic islands. *Environ. Model. Software* 140, 105015. <https://doi.org/10.1016/j.envsoft.2021.105015>.
- Mattsson, K., Johnson, E.V., Malmendal, A., Linse, S., Hansson, L.-A., Cedervall, T., 2017. Brain damage and behavioural disorders in fish induced by plastic nanoparticles delivered through the food chain. *Sci. Rep.* 7, 11452. <https://doi.org/10.1038/s41598-017-10813-0>.
- McCarthy, A.H., Peck, L.S., Aldridge, D.C., 2022. Ship traffic connects Antarctica's fragile coasts to worldwide ecosystems. *Proc. Natl. Acad. Sci.* 119, e2110303118 <https://doi.org/10.1073/pnas.2110303118>.
- Meides, N., Mauel, A., Menzel, T., Altstädt, V., Ruckdäschel, H., Senker, J., Strohriegel, P., 2022. Quantifying the fragmentation of polypropylene upon exposure to accelerated weathering. *Microplastics and Nanoplastics* 2, 23. <https://doi.org/10.1186/s43591-022-00042-2>.
- Menzel, T., Meides, N., Mauel, A., Mansfeld, U., Kretschmer, W., Kuhn, M., Herzog, E.M., Altstädt, V., Strohriegel, P., Senker, J., Ruckdäschel, H., 2022. Degradation of low-density polyethylene to nanoplastic particles by accelerated weathering. *Sci. Total Environ.* 826, 154035 <https://doi.org/10.1016/j.scitotenv.2022.154035>.
- Miklasz, K.A., Denny, M.W., 2010. Diatom sinkings speeds: improved predictions and insight from a modified Stokes' law. *Limnol. Oceanogr.* 55, 2513–2525. <https://doi.org/10.4319/lo.2010.55.6.2513>.
- Mishra, A.K., Singh, J., Mishra, P.P., 2021. Microplastics in polar regions: An early warning to the world's pristine ecosystem. *Sci. Total Environ.* 784, 147149 <https://doi.org/10.1016/j.scitotenv.2021.147149>.
- Moon, S., Martin, L.M.A., Kim, S., Zhang, Q., Zhang, R., Xu, W., Luo, T., 2024. Direct observation and identification of nanoplastics in ocean water. *Sci. Adv.* 10, eadh1675 <https://doi.org/10.1126/sciadv.adh1675>.
- Morrison, A.K., Hogg, A.M.C., England, M.H., Spence, P., 2020. Warm circumpolar deep water transport toward Antarctica driven by local dense water export in canyons. *Sci. Adv.* 6, eaav2516 <https://doi.org/10.1126/sciadv.aav2516>.
- Mountford, A.S., Maqueda, M.A.M., 2021. Modeling the accumulation and transport of microplastics by sea ice. *J. Geophys. Res.: Oceans* 126, e2020JC016826. <https://doi.org/10.1029/2020JC016826>.
- Munari, C., Infantini, V., Scoptoni, M., Rastelli, E., Corinaldesi, C., Mistri, M., 2017. Microplastics in the sediments of Terra Nova Bay (Ross Sea, Antarctica). *Mar. Pollut. Bull.* 122, 161–165. <https://doi.org/10.1016/j.marpolbul.2017.06.039>.
- Naveira Garabato, A.C., Zika, J.D., Jullion, L., Brown, P.J., Holland, P.R., Meredith, M.P., Bacon, S., 2016. The thermodynamic balance of the Weddell gyre. *Geophys. Res. Lett.* 43, 317–325. <https://doi.org/10.1002/2015GL066658>.
- Nøst, O.A., Bjuw, M., Tverberg, V., Lydersen, C., Hattermann, T., Zhou, Q., Smedsrud, L.H., Kovacs, K.M., 2011. Eddy overturning of the Antarctic Slope Front controls glacial melting in the Eastern Weddell Sea. *J. Geophys. Res.: Oceans* 116. <https://doi.org/10.1029/2011JC006965>.
- Obbard, R.W., Sadri, S., Wong, Y.Q., Khitun, A.A., Baker, I., Thompson, R.C., 2014. Global warming releases microplastic legacy frozen in Arctic Sea ice. *Earth's Future* 2, 315–320. <https://doi.org/10.1002/2014EF000240>.
- Pabortsava, K., Lampitt, R.S., 2020. High concentrations of plastic hidden beneath the surface of the Atlantic Ocean. *Nat. Commun.* 11, 4073. <https://doi.org/10.1038/s41467-020-17932-9>.
- Pakhomova, S., Berezina, A., Lusher, A.L., Zhdanov, I., Silvestrova, K., Zavalov, P., van Bavel, B., Yakushev, E., 2022. Microplastic variability in subsurface water from the Arctic to Antarctica. *Environ. Pollut.* 298, 118808 <https://doi.org/10.1016/j.envpol.2022.118808>.
- Pauthenet, E., Sallée, J.-B., Schmidtko, S., Nerini, D., 2021. Seasonal variation of the Antarctic slope front occurrence and position estimated from an interpolated hydrographic climatology. *J. Phys. Oceanogr.* 51, 1539–1557. <https://doi.org/10.1175/JPO-D-20-0186.1>.
- Peck, L.S., 2018. Antarctic marine biodiversity: Adaptations, environments and responses to change. In: Evans, A.J., Dale, A.C., Firth, L.B., Smith, I.P. (Eds.), *Hawkins, S.J. CRC Press, Oceanography and Marine Biology*, pp. 105–236. <https://doi.org/10.1201/9780429454455-3>.
- Peeken, I., Primpke, S., Beyer, B., Gütermann, J., Katlein, C., Krumpfen, T., Bergmann, M., Hehemann, L., Gerdts, G., 2018. Arctic Sea ice is an important temporal sink and means of transport for microplastic. *Nat. Commun.* 9, 1505. <https://doi.org/10.1038/s41467-018-03825-5>.
- Pörtner, H.O., 2006. Climate-dependent evolution of Antarctic ectotherms: An integrative analysis. *Deep Sea Research Part II: Topical Studies in Oceanography, EASIZ: Ecology of the Antarctic Sea Ice Zone* 53, 1071–1104. <https://doi.org/10.1016/j.dsr2.2006.02.015>.
- Poulain, M., Mercier, M.J., Brach, L., Martignac, M., Routaboul, C., Perez, E., Desjean, M.C., Halle, A. ter, 2018. Small microplastics as a Main contributor to plastic mass balance in the North Atlantic subtropical gyre. *Environ. Sci. Technol.* <https://doi.org/10.1021/acs.est.8b05458>.
- Primpke, S., Wirth, M., Lorenz, C., Gerdts, G., 2018. Reference database design for the automated analysis of microplastic samples based on Fourier transform infrared (FTIR) spectroscopy. *Anal. Bioanal. Chem.* 410, 5131–5141. <https://doi.org/10.1007/s00216-018-1156-x>.
- Primpke, S., Dias, P.A., Gerdts, G., 2019. Automated identification and quantification of microfibrils and microplastics. *Anal. Methods* 11, 2138–2147. <https://doi.org/10.1039/C9AY00126C>.

- Primpke, S., Cross, R.K., Mintenig, S.M., Simon, M., Vianello, A., Gerdts, G., Vollertsen, J., 2020. Toward the systematic identification of microplastics in the environment: evaluation of a new independent software tool (siMPle) for spectroscopic analysis. *Appl. Spectrosc.* 74, 1127–1138. <https://doi.org/10.1177/0003702820917760>.
- Primpke, S., Meyer, B., Falcou-Préfol, M., Schütte, W., Gerdts, G., 2024. At second glance: the importance of strict quality control – a case study on microplastic in the Southern Ocean key species Antarctic krill. *Euphausia superba*. *Sci. Total Environ.* 918, 170618 <https://doi.org/10.1016/j.scitotenv.2024.170618>.
- Quinn, B., Murphy, F., Ewins, C., 2017. Validation of density separation for the rapid recovery of microplastics from sediment. *Anal. Methods* 9, 1491–1498. <https://doi.org/10.1039/C6AY02542K>.
- R Core Team, 2023. R: A Language and Environment for Statistical Computin. R Foundation for Statistical Computing, Vienna, Austria. <https://www.R-project.org/>.
- Roscher, L., Fehres, A., Reisel, L., Halbach, M., Scholz-Böttcher, B., Gerriets, M., Badewien, T.H., Shiravani, G., Wurpts, A., Primpke, S., Gerdts, G., 2021. Microplastic pollution in the Weser estuary and the German North Sea. *Environ. Pollut.* 288, 117681 <https://doi.org/10.1016/j.envpol.2021.117681>.
- Roscher, L., Halbach, M., Nguyen, M.T., Hebler, M., Lushtinetz, F., Scholz-Böttcher, B. M., Primpke, S., Gerdts, G., 2022. Microplastics in two German wastewater treatment plants: year-long effluent analysis with FTIR and Py-GC/MS. *Sci. Total Environ.* 817, 152619 <https://doi.org/10.1016/j.scitotenv.2021.152619>.
- Rota, E., Bergami, E., Corsi, I., Bargagli, R., 2022. Macro- and microplastics in the Antarctic environment: ongoing assessment and perspectives. *Environments* 9, 93. <https://doi.org/10.3390/environments9070093>.
- Rowlands, E., Galloway, T., Cole, M., Lewis, C., Peck, V., Thorpe, S., Manno, C., 2021. The Effects of Combined Ocean Acidification and Nanoplastic Exposures on the Embryonic Development of Antarctic Krill. *Front. Mar. Sci.*, p. 8.
- Sfriso, A.A., Tomio, Y., Rosso, B., Gambaro, A., Sfriso, A., Corami, F., Rastelli, E., Corinaldesi, C., Mistri, M., Munari, C., 2020. Microplastic accumulation in benthic invertebrates in Terra Nova Bay (Ross Sea, Antarctica). *Environ. Int.* 137, 105587 <https://doi.org/10.1016/j.envint.2020.105587>.
- Shamskhany, A., Karimpour, S., 2022. Entrainment and vertical mixing of aquatic microplastics in turbulent flow: the coupled role of particle size and density. *Mar. Pollut. Bull.* 184, 114160 <https://doi.org/10.1016/j.marpolbul.2022.114160>.
- Sökmen, T.Ö., Sulukan, E., Türkoğlu, M., Baran, A., Özkaraca, M., Ceyhun, S.B., 2020. Polystyrene nanoplastics (20 nm) are able to bioaccumulate and cause oxidative DNA damages in the brain tissue of zebrafish embryo (*Danio rerio*). *NeuroToxicology* 77, 51–59. <https://doi.org/10.1016/j.neuro.2019.12.010>.
- Song, Y.K., Hong, S.H., Jang, M., Kang, J.-H., Kwon, O.Y., Han, G.M., Shim, W.J., 2014. Large accumulation of Micro-sized synthetic polymer particles in the sea surface microlayer. *Environ. Sci. Technol.* 48, 9014–9021. <https://doi.org/10.1021/es501757s>.
- Strobel, A., Burkhardt-Holm, P., Schmid, P., Segner, H., 2015. Benzo(a)pyrene metabolism and EROD and GST biotransformation activity in the liver of red- and White-blooded Antarctic fish. *Environ. Sci. Technol.* 49, 8022–8032. <https://doi.org/10.1021/acs.est.5b00176>.
- Suaría, G., Perold, V., Lee, J.R., Lebourd, F., Aliani, S., Ryan, P.G., 2020. Floating macro- and microplastics around the Southern Ocean: results from the Antarctic circumnavigation expedition. *Environ. Int.* 136, 105494 <https://doi.org/10.1016/j.envint.2020.105494>.
- Sullivan, T.N., Wang, B., Espinosa, H.D., Meyers, M.A., 2017. Extreme lightweight structures: avian feathers and bones. *Mater. Today* 20, 377–391. <https://doi.org/10.1016/j.mattod.2017.02.004>.
- Sun, Y., Xu, W., Gu, Q., Chen, Y., Zhou, Q., Zhang, L., Gu, L., Huang, Y., Lyu, K., Yang, Z., 2019. Small-Sized Microplastics Negatively Affect Rotifers: Changes in the Key Life-History Traits and Rotifer–Phaeocystis Population Dynamics. *Environ. Sci. Technol.* 53, 9241–9251. doi:<https://doi.org/10.1021/acs.est.9b02893>.
- Tagg, A., Harrison, J.P., Ju-Nam, Y., Sapp, M., Bradley, E.L., Sinclair, C.J., Ojeda, J.J., 2017. Fenton's reagent for the rapid and efficient isolation of microplastics from wastewater. *Chem. Commun.* 53, 372–375. <https://doi.org/10.1039/C6CC08798A>.
- Thompson, A.F., Stewart, A.L., Spence, P., Heywood, K.J., 2018. The Antarctic slope current in a changing climate. *Rev. Geophys.* 56, 741–770. <https://doi.org/10.1029/2018RG000624>.
- Van Cauwenberghe, L., Vanreusel, A., Mees, J., Janssen, C.R., 2013. Microplastic pollution in deep-sea sediments. *Environ. Pollut.* 182 <https://doi.org/10.1016/j.envpol.2013.08.013>.
- Vernet, M., Geibert, W., Hoppema, M., Brown, P.J., Haas, C., Hellmer, H.H., Jokat, W., Jullion, L., Mazloff, M., Bakker, D.C.E., Brearley, J.A., Croot, P., Hattermann, T., Hauck, J., Hillenbrand, C.-D., Hoppe, C.J.M., Huhn, O., Koch, B.P., Lechtenfeld, O.J., Meredith, M.P., Naveira Garabato, A.C., Nöthig, E.-M., Peeken, I., Rutgers van der Loeff, M.M., Schmidt, S., Schröder, M., Strass, V.H., Torres-Valdés, S., Verdy, A., 2019. The Weddell gyre, Southern Ocean: present knowledge and future challenges. *Rev. Geophys.* 57, 623–708. <https://doi.org/10.1029/2018RG000604>.
- von Moos, N., Burkhardt-Holm, P., Köhler, A., 2012. Uptake and effects of microplastics on cells and tissue of the blue mussel *Mytilus edulis* L. after an experimental exposure. *Environ. Sci. Technol.* 46, 11327–11335. <https://doi.org/10.1021/es302332w>.
- Waller, C.L., Griffiths, H.J., Waluda, C.M., Thorpe, S.E., Loiza, I., Moreno, B., Pachterres, C.O., Hughes, K.A., 2017. Microplastics in the Antarctic marine system: An emerging area of research. *Sci. Total Environ.* 598, 220–227. <https://doi.org/10.1016/j.scitotenv.2017.03.283>.
- Wang, Fei, Li, S., Peng, L., Wang, Fen, Zeng, E.Y., 2024. Chapter 5 - sorption of toxic chemicals on microplastics. In: Zeng, E.Y. (Ed.), *Microplastic Contamination in Aquatic Environments*, Second edition. Elsevier, pp. 113–139. <https://doi.org/10.1016/B978-0-443-15332-7.00011-9>.
- Wilkie Johnston, L., Bergami, E., Rowlands, E., Manno, C., 2023. Organic or junk food? Microplastic contamination in Antarctic krill and salps. *R. Soc. Open Sci.* 10, 221421 <https://doi.org/10.1098/rsos.221421>.
- Witzig, C.S., Földi, C., Wörle, K., Habermehl, P., Pittroff, M., Müller, Y.K., Lauschke, T., Fiener, P., Dierkes, G., Freier, K.P., Zumbülte, N., 2020. When Good Intentions Go Bad—False Positive Microplastic Detection Caused by Disposable Gloves. *Environ. Sci. Technol.* 54, 12164–12172. <https://doi.org/10.1021/acs.est.0c03742>.
- Front matter. In: Wypych, G. (Ed.), 2012. *Handbook of Polymers*. Elsevier, Oxford, p. i. <https://doi.org/10.1016/B978-1-895198-47-8.50001-1>.
- Zhang, M., Liu, S., Bo, J., Zheng, R., Hong, F., Gao, F., Miao, X., Li, H., Fang, C., 2022. First evidence of microplastic contamination in Antarctic fish (Actinopterygii, Perciformes). *Water* 14, 3070. <https://doi.org/10.3390/w14193070>.
- Zhang, S., Zhang, W., Ju, M., Qu, L., Chu, X., Huo, C., Wang, J., 2022. Distribution characteristics of microplastics in surface and subsurface Antarctic seawater. *Sci. Total Environ.* 838, 156051 <https://doi.org/10.1016/j.scitotenv.2022.156051>.
- Zhang, W., Hao, Q., Zhu, J., Deng, Y., Xi, M., Cai, Y., Liu, C., Zhai, H., Le, F., 2023. Nanoplanktonic Diatom Rapidly Alters Sinking Velocity Via Regulating Lipid Content and Composition in Response to Changing Nutrient Concentrations. *Front. Mar. Sci.*, p. 10.
- Zhu, W., Liu, W., Chen, Y., Liao, K., Yu, W., Jin, H., 2023. Microplastics in Antarctic krill (*Euphausia superba*) from Antarctic region. *Sci. Total Environ.* 870, 161880 <https://doi.org/10.1016/j.scitotenv.2023.161880>.